PB89-169858

Annular Denuder Sampler for Phase-Distributed Semivolatile Organic Chemicals

Battelle Columbus Div., OH

Prepared for

Environmental Protection Agency
Research Triangle Park, NC

Mar 89

U.S. Department of Commerce
National Technical Information Service

TECHNICAL REPORT DATA (Please read Instructions on the reverse before completing)		
1. REPORT NO. EPA/600/3-89/029	2.	3. RECIPIENT'S ACCESSION NO. PB89 169858/AS
4. TITLE AND SUBTITLE ANNULAR DENUDER SAMPLER FOR PHASE-DISTRIBUTED SEMIVOLATILE ORGANIC CHEMICALS		5. REPORT DATE March 1989 6. PERFORMING ORGANIZATION CODE
7. AUTHOR(S) R. W. Coutant, P. J. Callahan and J. C. Chuang		8. PERFORMING ORGANIZATION REPORT NO.
9. PERFORMING ORGANIZATION NAME AND ADDRESS BATTELLE COLUMBUS DIVISION 505 KING AVENUE COLUMBUS, OH 43201-2693		10. PROGRAM ELEMENT NO. 11. CONTRACT/GRANT NO. EPA 68-02-4127
12. SPONSORING AGENCY NAME AND ADDRESS U.S. ENVIRONMENTAL PROTECTION AGENCY ATMOSPHERIC RESEARCH & EXPOSURE ASSESSMENT LAB/RTP METHODS RESEARCH AND DEVELOPMENT DIVISION, MRB RESEARCH TRIANGLE PARK, NC 27711		13. TYPE OF REPORT AND PERIOD COVERED Project Report 3/87-9/88 14. SPONSORING AGENCY CODE EPA/600/09
15. SUPPLEMENTARY NOTES		

16. ABSTRACT

A compact compound annular denuder, with a removal efficiency for volatile polynuclear aromatic hydrocarbons (PAH) of at least 90 percent at flow rates of up to 200 L/min, was designed for use with the PS-1 sampler. Laboratory tests of this denuder showed no detectable (< 10 percent) removal of ambient particulate matter larger than 0.1 μm mean diameter at flow rates of 100-200 L/min. The vapor collection efficiency, as measured with naphthalene, was better than 95 percent, and the capacity for removal of approximately 180 μg of naphthalene was better than 90 percent.

The field experiments consisted of three series: (1) outdoors during the winter; (2) indoors within a laboratory; and (3) outdoors during the summer. In these experiments a denuder difference approach was followed to monitor the phase distributions of 18 PAH. The 2-, 3-, and 4-ring PAH all showed considerable potential for volatilization, but no evidence (< 0.02 ng/m^3) was seen for the heavier PAH in the vapor phase. The results in general are consistent with previous work and extend the overall body of information on the phase distributions of PAH and their tendencies for artifact formation as a result of volatilization during sampling. Phase distributions for PAH were shown to be well represented by the Dubrinin-Radushkevich isotherm under both summer and winter conditions.

17. KEY WORDS AND DOCUMENT ANALYSIS

a. DESCRIPTORS	b. IDENTIFIERS/OPEN ENDED TERMS	c. COSATI Field/Group

18. DISTRIBUTION STATEMENT	19. SECURITY CLASS (This Report)	21. NO. OF PAGES
RELEASE TO PUBLIC	UNCLASSIFIED	109
	20. SECURITY CLASS (This page) UNCLASSIFIED	22. PRICE

EPA Form 2220-1 (Rev. 4-77) PREVIOUS EDITION IS OBSOLETE

PB89-169858

EPA/600/3-89/029
March 1989

ANNULAR DENUDER SAMPLER FOR PHASE-DISTRIBUTED SEMIVOLATILE ORGANIC CHEMICALS

by

R. W. Coutant, P. J. Callahan and J. C. Chuang
Battelle Columbus Division
Columbus, Ohio 43201

Contract No. 68-02-4127

Project Officer

Robert G. Lewis
Atmospheric Research and Exposure Assessment Laboratory
U.S. Environmental Protection Agency
Research Triangle Park, NC 27711

ATMOSPHERIC RESEARCH AND EXPOSURE ASSESSMENT LABORATORY
U.S. ENVIRONMENTAL PROTECTION AGENCY
RESEARCH TRIANGLE PARK, NC 27711

REPRODUCED BY
U.S. DEPARTMENT OF COMMERCE
NATIONAL TECHNICAL INFORMATION SERVICE
SPRINGFIELD, VA. 22161

DISCLAIMERS

This report is a work prepared for the United States by Battelle. In no event shall either the United States or Battelle have any responsibility or liability for any consequences of any use, misuse, inability to use, or reliance upon the information contained herein, nor does either warrant or otherwise represent in any way the accuracy, adequacy, efficacy, or applicability of the contents hereof.

The information in this document has been funded wholly or in part by the United States Environmental Protection Agency under Contract No. 68-02-4127 to Battelle Columbus Division. It has been subjected to the Agency's peer and administrative review, and it has been approved for publication as an EPA document. Mention of trade names or commercial products does not constitute endorsement or recommendation for use.

FOREWORD

Measurement and monitoring research efforts are designed to anticipate environmental problems, to support regulatory actions by developing an indepth understanding of the nature and processes that impact health and the ecology, to provide innovative means of monitoring compliance with regulations, and to evaluate the effectiveness of health and environmental protection efforts through monitoring of long-term trends. The Atmospheric Research and Exposure Assessment Laboratory, Research Triangle Park, North Carolina, has responsibility for: assessment of environmental monitoring technology and systems for air, implementation of agency-wide quality assurance programs for air pollution measurement systems, and supplying technical support to other groups in the Agency including the Office of Air and Radiation, the Office of Toxic Substances, and the Office of Solid Waste.

The determination of human exposure to semivolatile organic compounds is an area of increasing importance to EPA. The fact that such compounds can be present in the atmosphere partly as free vapors and partly in adsorbed states on ambient particulate matter is significant with respect to their transport and fate in the atmosphere and to the mechanism and extent of their uptake during respiration. The compound annular denuder system and the field experiments described in this report represent a significant step in providing capability for distinguishing between vapor phase and adsorbed semivolatile organic compounds when using the high sampling rates that are necessary for detection of many such compounds that are present at only trace levels in the environment.

Gary J. Foley
Director
Atmospheric Research and Exposure Assessment Laboratory
Research Triangle Park, North Carolina, 27711

ABSTRACT

The objectives of this study were (1) to design and construct a high-efficiency, high-volume denuder sampler to separately collect and maintain the integrities of the vapor and particle-associated fractions of organic chemicals that may be phase distributed in the atmosphere; and (2) to use this apparatus in a series of field measurements to determine the phase distributions of selected polynuclear aromatic hydrocarbons.

The design approach involved consideration of diffusive mass transport and the physical limitations of the standard General Metal Works PS-1 high-volume sampler. The goal was to achieve a compact denuder, with a removal efficiency for volatile PAH of at least 90 percent at flow rates of up to 200 L/min, which could readily be coupled to the PS-1 sampler. The result is a 20.3 cm x 8.25 cm compound annular denuder consisting of a solid aluminum core plus 12 concentric cylindrical aluminum shells, with annuli thicknesses of 1.6 mm. The shells are coated with approximately 30μm-thick layers of silicone grease that serves as the vapor phase collector. Laboratory tests of this denuder show no detectable (<10 percent) removal of ambient particulate matter larger than 0.1 μm mean diameter at flow rates of 100-200 L/min. The vapor collection efficiency, as measured with naphthalene, is better than 95 percent, and the denuder has the capacity for removal of approximately 180 μg of naphthalene with better than 90 percent efficiency.

The field experiments consisted of three series: (1) outdoors during the winter; (2) indoors within a laboratory; and (3) outdoors during the summer. In these experiments, a denuder difference approach was followed to monitor the phase distributions of 18 PAH: naphthalene, quinoline, acenaphthylene, anthracene, phenanthrene, pyrene, fluoranthene, cyclopenta(c,d,)pyrene, benz(a)anthracene, chrysene, retene, benzo(a)pyrene, benzo(e)pyrene, benzofluoranthene, perylene, benzo(g,h,i)perylene, indeno(1,2,3-c,d)pyrene, and coronene. The 2-, 3-, and 4-ring PAH all showed considerable potential for volatilization, but no evidence (<0.02 ng/m^3) was seen for the heavier PAH in the vapor phase. The results in general are consistent with previous work and extend the overall body of information on the phase distributions of PAH and their tendencies for artifact formation as a result of volatilization during sampling.

This report is being submitted in fulfillment of Contract No. 68-02-4127 (WA-41 and WA-46) by Battelle Columbus Division under the sponsorship of the U.S. Environmental Protection Agency. It covers a period of March 1, 1987, to September 30, 1988, and work was completed as of September 30, 1988.

CONTENTS

Disclaimer ii

Foreword iii

Abstract iv

Figures vi

Tables vii

1. Introduction 1

2. Objective 3

3. Conclusions and Recommendations 4

4. Experimental Methods and Results 6
   Experimental Procedures 6
   Results 12

References 33

Appendices

A. Annular Denuder Design (paper prepared for publication) 35
B. PAH Sampling Data 71

FIGURES

Number		Page
1	Dependence of Artifact Formation on PAH Volatility	17
2	Composition of Volatile PAH in Total Sample. (Normalized to Phenanthrene)	19
3	Composition of Volatile PAH in Adsorbed Phase. (Normalized to Phenanthrene)	20
4	Dubinin-Radushkevich Plot for Phenanthrene	22
5	Dubinin-Radushkevich Plot for Fluoranthene	23
6	Dubinin-Radushkevich Plot for Anthracene	24
7	Dubinin-Radushkevich Plot for Pyrene	25
8	Dubinin-Radushkevich Plot for Benz(a)anthracene	26
9	Dubinin-Radushkevich Plot for Chrysene	27
10	Dubinin-Radushkevich Plot for Retene	28
11	Generalized Dubinin-Radushkevich Plot for Volatile PAH	30
12	Generalized PAH Vapor Concentrations	32

TABLES

Number		Page
1	GC and MS Operation Conditions	11
2	Summary of Field Blanks	13
3	Summary of PAH Vapor and Artifact Levels Determined with both OTD and HVCAD Samplers.	15
4	Preliminary Dubinin-Radushkevich Parameters	21
5	Recommended Dubinin-Radushkevich Parameters	29

SECTION 1

INTRODUCTION

Many polynuclear aromatic hydrocarbons (PAH) are known or suspected carcinogens. The determination of concentrations of PAH in ambient air is, therefore, of considerable importance to the characterization of air quality. The task of sampling PAH is complicated by the fact that many PAH have equilibrium vapor concentrations that are considerably higher than their normal ambient air concentrations. This implies a temperature- and concentration-dependent distribution of such PAH between particulate and vapor phases, and also suggests the possibility for artifact occurrence due to volatilization during the sampling process (Junge, 1977).

From the viewpoints of atmospheric fate and transport and, more importantly, human health risk assessment, it may be necessary to distinguish between the vapor and particle-bound PAH. Traditional sampling methods have used only filtration to collect ambient aerosol. More recently, the use of backup traps containing polyurethane foam (PUF) or other vapor sorbents such as XAD-2 to collect vapor passing through the filter has become more widespread (e.g. Yamasaki et al. 1982; Van Vaeck et al. 1984). While this approach may permit total collection of PAH, it does not take into account the possibility of artifact formation as a result of either condensation or vaporization during the sampling process. Furthermore, there is the possibility that the integrity of collected samples may be altered by reaction of PAH with reactive species such as ozone during sampling. Other researchers have used vapor denuder systems to examine the questions of carbonaceous particle integrity and sampling of chlorinated organic compounds (Lane et al. 1988).

In two previous work assignments conducted under this contract, a research-level denuder sampler was used to evaluate the phase distributions of selected PAH during ambient air sampling. Results of that work were published recently (Coutant et al. 1988). The denuder used in that study was of an open tubular design that limited the sampling rate to only 15 L/min, a rate well below the 200 L/min normally used for ambient air sampling with the PS-1 sampler. Many PAH and other semivolatile organic compounds (SVOC) are present in ambient air at levels that are low enough to require the use of the larger sampling rate to provide enough sample for analytical and bioassay purposes. A

practical denuder sampler for PAH and other SVOC therefore requires the use of a more efficient denuder system that will permit sampling at rates of the order of 100-200 L/min.

A paper describing the design, construction and preliminary laboratory evaluation of a high volume compound annular denuder (HVCAD) sampler that satisfies these needs has been prepared for publication in the open literature, and is attached for easy reference as Appendix A of this report.

SECTION 2

OBJECTIVES

The objectives of WA-41 were to design and construct a high-efficiency, high-volume denuder sampler that would separately collect and maintain the integrities of the vapor and particle-associated fractions of organic chemicals that are phase-distributed in the atmosphere. The specific goal was to construct a compact denuder that could be readily integrated within the normal PS-1 sampler structure, while achieving at least 90 percent removal efficiency for SVOC vapors at a sampling rates up to 200 L/min. Additionally, this device should not interfere with normal filtration sampling of ambient particulate matter.

The objective of WA-46 was to utilize this high efficiency denuder sampler in a series of denuder difference type experiments to determine the phase distribution of selected polynuclear aromatic hydrocarbons in the ambient air. These field experiments were to include measurements made during both winter and summer months to attempt to encompass the normal range of ambient PAH sampling conditions.

SECTION 3

CONCLUSIONS AND RECOMMENDATIONS

A denuder sampler capable of operating at a minimum of 95 percent vapor removal efficiency at flow rates up to 200 L/min was designed and constructed. This denuder is compact (20.3 cm x 8.25 cm) and couples readily to the PS-1 sampler. Its holder serves as an interface to the PS-1 sampler and as a transport container. Laboratory tests of this denuder show no detectable (<10 percent) removal of ambient particulate matter larger than 0.1 μm mean diameter at flow rates of 100-200 L/min. The vapor collection efficiency, as measured with naphthalene, is better than 95 percent, and the denuder has the capacity for removal of approximately 180 μg of naphthalene with better than 90 percent efficiency.

Use of the sampler in a series of outdoor and indoor denuder difference sampling experiments yielded phase distribution data that are consistent with our previous work. The results show that 2-, 3-, and 4-ring PAH are sufficiently volatile that measurable quantities of these compounds are found in the vapor phase. Also, these same compounds show considerable tendencies for volatilization as a consequence of changes in ambient conditions during the sampling process. This sampling artifact is shown to be correlated with the vapor pressures of the PAH. The dependence of PAH distribution between vapor and adsorbed states is shown to be well-represented by the Dubinin-Radushkevich isotherm. As a rule-of-thumb, ambient PAH vapor concentrations are approximately 1/10,000 th of the equilibrium vapor concentrations of the pure compounds. Limited data on quinoline obtained in this study suggest lower vapor concentrations for this polar PAH. While the normalized concentrations (using phenanthrene as a reference) of volatile PAH in ambient air appear to vary some with the seasons, the normalized concentrations of the same compounds in the adsorbed phase appear to be relatively constant. Seasonal variations in the relative amounts of some of the volatile PAH such as acenaphthylene and pyrene may be due to the reactivity of these compounds.

The denuder design and performance model developed in this program provides a sophisticated, but easy to use, mechanism for extending the current annular denuder design to other sampling needs and applications. For example,

the design of a compact compound annular denuder for use with low-volume indoor samplers would be quite straightforward.

It is recommended that consideration be given to the phase distributions of other types of SVOC than the PAH included in this study. Such compounds as the polar PAH and pesticides would be expected to be more strongly adsorbed than the compounds studied here. While, in principle, the Dubinin-Radushkevich isotherm should apply to such compounds, with appropriate corrections for their polarizability, other generalizations derived from the current work, such as the relationship between artifact and vapor pressure, may not apply.

SECTION 4

EXPERIMENTAL METHODS AND RESULTS

EXPERIMENTAL PROCEDURES

Denuder Preparation

The denuder assembly was constructed of a solid aluminum core plus 12 concentric aluminum tubes held in place by a three-armed radial rake at each end. Removal of a single wing-nut facilitated disassembly of the denuder for cleaning and recoating. Earlier work (WA-41) had shown that recoating was advisable after each use of the denuder because of air oxidation of the silicone surface. Examination of the surface using ESCA showed appreciable oxidation (ca. 30 percent) of the top 30 Å in a period of 30 days, but no detectable oxidation over a 1 - 2 day period.

Before being coated, the HVCAD was cleaned to remove the previous silicone grease coating. Each of the HVCAD tubes was first immersed in a bath of fresh dichloromethane for at least 15 hours. The tubes were then removed from the bath and wiped with paper wipes. Next the tubes were placed in another bath of fresh dichloromethane for at least 1 hour. After this time period, the tubes were removed from the bath, wiped off, and then allowed to dry.

After cleaning, each HVCAD tube was weighed to the nearest 0.01 g. The weight of each tube was then compared to its previous uncoated weight to determine if it was sufficiently clean.

The clean tubes were coated with a solution of Dow Corning high vacuum silicone grease dissolved in dichloromethane. Typically the concentration of this solution was 150 g of grease in 380 ml of dichloromethane. The tubes were coated by placing them one at a time in a sealed 1/2 gallon polyethylene jug that contained 400-600 ml of coating solution. The jug was rotated back and forth for approximately one minute until all of the tube surface was coated. The tube was then removed from the jug and allowed to dry on a drying rack.

After being coated, the tubes were weighed to the nearest 0.01 g to estimate the thickness of the coating. The HVCAD was then assembled, and 60 ml/min of nitrogen gas was passed through it for 30 minutes to remove any remaining dichloromethane from the coating.

Filters

The filters used for the sampling trials were 104 mm QATP (quartz fiber) filters obtained from Pallflex. These filters were baked at 450 C for 6 hours before being stored individually between similarly treated watchglasses that were sealed with Teflon tape.

Polyurethane Foam (PUF) Cartridges

The PS-1 glass cartridges and aluminum foil used for wrapping clean cartridges were cleaned by heating in a muffle oven at 400°C for 16 hours.

PUF plugs were cleaned by compression rinsing using 50 cycles in acetone followed by 50 cycles in 800 ml toluene and 50 cycles in 10 percent ether in hexane. The PUF plugs were then placed into the clean PS-1 glass cartridges, extracted in a Soxhlet extractor with 10 percent ether in hexane for 16 hours, and were dried under vacuum at room temperature. After drying, each PUF cartridge was individually wrapped in clean aluminum foil and was stored in a glass jar closed with a Teflon-lined or aluminum foil-lined cap. Typically, PUF plugs were used within 48 hours after cleanup.

Sampling Trials

All sampling trials were conducted with two General Metal Works PS-1 samplers operated in parallel. One of the samplers was modified by lowering the pump mounting platform to provide room for the HVCAD above the filter holder. No changes were made to the pumping and sample collection assembly itself on the modified sampler.

On both PS-1 samplers, dual sampling modules consisting of a filter and PUF cartridge were used for series collection of particulate-bound and vapor phase PAH. On the modified PS-1 sampler, the HVCAD was mounted ahead of

the dual sampling module to remove PAH vapor ahead of the filter. A threaded open fitting with inset O-ring was used to couple the HVCAD to the dual sampling module.

For each sampling trial, flow rates were measured with the use of a calibrated propeller-type anemometer. When flow measurements were taken, an 18 cm length of plastic pipe was used to couple the anemometer to the inlet end of the dual sampling module on one sampler and the HVCAD on the other sampler. For the winter and indoor trials, flow rates were measured on both samplers at the beginning and end of each sampling trial. For the summer trials, flow rates were typically measured on each sampler at the beginning, middle, and end of each sampling trial. The initial flow rates through each sampler were watched as closely as possible at about 100 L/min.

Air temperature was monitored for each trial with a thermocouple mounted near the two PS-1 samplers. This thermocouple was connected to a strip chart recorder to obtain a continuous record of air temperature. Also during each trial, a continuous record of the barometric pressure was kept by an automatic recording barometer. Measured flow rates were corrected to standard conditions using these data.

Sampling Protocol

Before each sampling trial, both PS-1 samplers were washed with dichloromethane. The metal portions of the dual sampling modules were also washed with dichloromethane, while the rubber gaskets of the modules were washed with methanol.

In loading the sampling modules for each trial, a fresh pair of cotton gloves was worn to transfer the PUF cartridge from the glass jar to the module. The caps were then replaced on the glass jars, and the caps rewrapped with electrical tape over Teflon tape. The filters were transferred from the watchglasses to the sampling modules with forceps. After loading, the filter watchglasses were resealed with electrical tape over Teflon tape.

Before each run was conducted, the weather reports were consulted to determine the probability of precipitation. Runs were made only when the chances of precipitation were minimal.

Two collection periods were used. Daytime trials were for 8 hours; nighttime trials were for 13 to 18 hours.

At the end of each sample run, the filters and PUF cartridges were removed from the dual sampling modules by the same procedures used for loading. After the filters had been resealed in the watchglasses, the encased filters were stored in a desiccator prior to being weighed and extracted. This desiccator was wrapped completely in aluminum foil to protect the filters from light. The glass jars containing the PUF cartridges were stored in a refrigerator prior to extraction. Extractions were carried out as soon as possible for each sample. For sampling runs that concluded early in the day, extractions were performed during that day; when the sampling runs ended late during the day, the filter and PUF samples were stored overnight before being extracted.

Field blanks were used to determine the extent of contamination of the filters and PUF cartridges during the loading and unloading process, and the measured blank levels were used to correct the observed filter and PUF analytical results. These field blank samples were carried through each step of the sampler setup process as though they were actually being used, but no air samples were drawn through them.

Data Analysis

The apparent vapor and artifact levels for each compound were calculated using the following equations:

$$F_{nd} = P - A_n \quad (1)$$

$$F_d = P - A_n - A_e \quad (2)$$

$$PUF_{nd} = V + A_n \quad (3)$$

$$PUF_d = (C/C_o)V + A_n + A_e \quad (4)$$

Here, F, PUF, P, V, and A refer to the amounts of each PAH associated with the filter, PUF, particulate, vapor, and artifact respectively. The subscripts d and nd denote denuder and non-denuder samplers, and subscripts n and e distinguish between the normal and excess artifact (that caused by the use of the denuder). The term C/C_o represents the average fraction of the

vapor that was not removed by the denuder, and this term was used to correct for the denuder inefficiency. This term was calculated for each specific run condition for each PAH using the finite-element computer model described in Appendix A. These calculations included correction of the diffusion coefficients of each compound to the average run temperature. Whenever possible the diffusion coefficients (at 25 C) used were taken from the literature. When this value was not available for a compound, it was estimated with the group contribution method of Fuller et al. (1966).

Raw run data and analytical data for these Work Assignments (41 and 46) are recorded in Battelle Laboratory Notebook Nos. 42460, 42882 and 43331. Spreadsheets containing the processed data are stored on floppy disks at Battelle Columbus Division.

Analysis

Gas chromatography/electron impact mass spectrometry (GC/EI-MS) was used to determine selected PAH and quinoline. A Finnigan TSQ 4500 GC/MS/MS was used and was operated in the GC/MS mode. Helium was used as the carrier gas as well as the reagent gas. A bonded-phase fused silica capillary column, HP Ultra No. 2 crosslinked 5 percent phenylmethylsilicone, was used as the GC column. The outlet of the GC column was located at the inlet of the MS ionization source. Data acquisition and processing were performed with a Finnigan INCOS Model 2300 data system. The GC and MS operating conditions are listed in Table 1.

Mass spectral intensities for the calibration compound perfluorotributylamine were generated daily and these intensities were used to verify that the fine balance tuning of the mass spectrometer had not varied significantly during the analysis of the sample extracts.

The standard solutions containing the target compounds were analyzed by GC/EI-MS in the multiple ion detection (MID) mode to determine the calibration curves. The internal standard, 9-phenylanthracene, was added to the standard solutions and the sample extracts at constant concentration levels (0.5 ng/μl) prior to analysis. Ion peaks monitored by MS were the molecular ion peaks (M) and the (M+1) peaks of the target compounds. The sample extracts were analyzed concurrently with the standard solutions. Identification of the

target compounds in the sample extracts was based on the correct molecular ion and the correct retention times. The response factor for each target compound relative to the internal standard was calculated from the standard

Table 1. GC and MS Operation Conditions

Chromatography	
Column:	HP Ultra No. 2 crosslinked 5 percent phenyl-methylsilicone 25 m x 0.20 mm, 0.11 μm film thickness
Carrier:	Helium
Carrier linear flow velocity:	30 cm/sec at 200 C
Injection volume:	1 μl
Injection mode:	splitless
Temperature Program	
Initial column temperature:	50 C
Initial hold time:	2 min
Program rate:	120 C (3.5 min) to 290 at 10 C/min
Final hold time:	10 min
Mass Spectrometer	
Ionization:	70 ev
Filament emission current:	0.3 ma
Preamplifier:	10^{-8} amp/volt
Electron multiplier gain:	10^{5}

analyses. Quantification of each target compound was based on the following equation:

$$C_X(ng/m^3) = \frac{A_S \times C_{is} \times F_V}{A_{is} \times Rf \times V}$$

where

C_X = Concentration of the target compound found in the air sampled, ng/m^3

A_S = Area count of the target compound

C_{is} = Concentration of the internal standard, 1 $ng/\mu l$

A_{is} = Area count of the internal standard

Rf = Response factor of the target compound

F_V = Total volume of a sample extract, μl

V = volume of air sampled, m^3

RESULTS

Blanks

Table 2 shows a summary of the medians and ranges for the target PAH in the filter and PUF field blanks. For the most part, the blank contributions to the total filter and PUF samples were small, but the phenanthrene and naphthalene field blanks were appreciable. Comparison of the field blanks with an analytical method blank (no sample matrix) indicated that the source of the field blank contamination was in the handling process during simulation of field sample loading. The method blank showed detectable amounts of only naphthalene, phenanthrene, pyrene, and fluoranthene, with the levels of these compounds being approximately 0.02 (phenanthrene) to 0.5 (pyrene) times the levels found in the field blanks.

Table 2. Summary of Field Blanks

Compound	Filter, ng			PUF, ng		
	Range	Median	Percent of Sample (a)	Range	Median	Percent of Sample (a)
Naphthalene	8.2-24	9.8	36	29-66	50	3
Quinoline	0-37	0	NA(b)	0-23	0	NA
Acenaphthylene	0	0	NA	0	0	NA
Anthracene	0-5.5	0	NA	2-11	6.6	3.7
Phenanthrene	32-85	53	32	56-120	91	5.8
Pyrene	8.3-19	14	12	17-27	25	7
Fluoranthene	12-23	16	12	24-46	39	2.7
Cyclopenta(c,d)pyrene	0	0	NA	0	0	NA
Benz(a)anthracene	0-6.4	1.3	5.5	0-4.5	1.2	20
Chrysene	0-6.6	1.8	3.6	0-3.2	2.4	19
Retene	0	0	NA	0	0	NA
Benzo(a)pyrene	0	0	NA	0	0	NA
Benzo(e)pyrene	0	0	NA	0	0	NA
Benzofluoranthene	0	0	NA	0	0	NA
Perylene	0	0	NA	0	0	NA
Benzo(g,h,i)perylene	0	0	NA	0	0	NA
Indeno(1,2,3-c,d)-pyrene	0	0	NA	0	0	NA
Coronene	0	0	NA	0	0	NA

(a) Median of blank to sample ratio expressed as a percentage
(b) Not applicable; blank below detection limit

Phase Distribution

A preliminary analysis of the data obtained on this program showed good correspondence with data previously obtained with the research level open tubular denuder (OTD) sampler used on WA-18 (see reference 5). Because of this correspondence, the data from that task have been combined with the current data to provide as complete representation of PAH phase distribution data as possible. Complete tabulations of the filter and PUF data for each run, including the data from WA-18 (1985-1986) are given in Appendix B. All data tabulated in Appendix B are corrected for field blank contributions. The discussion below addresses information derived from that data.

The assumptions that both samplers collect identical amounts of particulate matter per unit volume of air sampled and that the true sample volumes are accurately known are critical to the denuder difference approach. In practice, there are always discrepancies between samples collected by collocated samplers. The relative average difference between the particulate catches of the denuder and non-denuder samplers was 3 percent for the current data and <1 percent for the previous data. However, relative differences for individual runs ranged from -33 percent to +38 percent. The raw data were, therefore, screened carefully. For most of the runs, the average particulate loading of the two samplers was used as a reference, but in cases where data from one of the samplers were obviously in error, the particulate loading of the other sampler was used as the reference. The processed data also were screened for other obvious errors. In a few cases, the apparent vapor or artifact levels were either greater than 100 percent or less than 0 percent of the total. Such data are not included in the discussions below.

Table 3 shows a summary of the percentages of each of the measured PAH found as either vapor or artifact.

Table 3. Summary of PAH Vapor and Artifact Levels Determined with both OTD and HVCAD Samplers (a)

Compound	Vapor		Artifact	
	Range	Median	Range	Median
Naphthalene(b,c)	9.1-47.3	22.4	47.1-89.8	75.5
Quinoline(c)	45.4-81	62.3	7.7-43.8	19.5
Acenaphthylene(c)	22.3-99.5	66.8	16.9-80.3	57.9
Anthracene	14.0-92.3	56.6	12.7-92.2	31.9
Phenanthrene	25.0-86.5	50.6	12.7-80.3	44.7
Pyrene	21.0-91.1	60.9	0.7-99.5	16.3
Fluoranthene	26.6-90	60.4	4.5-61.7	16.5
Cyclopenta(c,d)pyrene	(compound not consistently detected)			
Benz(a)anthracene	7.5-67.2	32.5	8.3-53.0	30.5
Chrysene	15.0-64.8	40.3	5.7-50.2	17.5
Retene(c)	30.7-92.3	78.1	3.3-21.1	7.4
Benzo(a)pyrene	ND(d)	ND	ND	ND
Benzo(e)pyrene	ND	ND	ND	ND
Benzofluoranthene	ND	ND	ND	ND
Perylene	ND	ND	ND	ND
Benzo(g,h,i)-perylene	ND	ND	ND	ND
Indeno(1,2,3-c,d)-pyrene	ND	ND	ND	ND
Coronene	ND	ND	ND	ND

(a) Expressed as percentage of total amount of each compound
(b) Some PUF data for naphthalene suspect because of possible breakthrough
(c) Compounds determined only in current series of experiments
(d) Not detected consistently in PUF samples

The data clearly show that the 2-, 3-, and 4-ring PAH are sufficiently volatile to be detected in the vapor phase, and that these same compounds can undergo phase change leading to artifact formation during the sampling process.

Artifact Formation

Assuming that the PAH in a parcel of ambient air is initially in an equilibrium distribution between absorbed and vapor phases, volatilization or condensation of adsorbed PAH during the sampling process can occur as a result of either of two possible changes in the ambient sampling conditions:

1. Changes in temperature can result in volatilization of previously collected particle-bound PAH.

2. Changes in the gross composition of the ambient air can expose the previously collected PAH to a different equilibrium condition, and thereby result in either volatilization or adsorption.

In most ambient sampling situations, temperatures are recorded as a part of the sampling protocol, but very little is known about the short term variations in the local PAH loading. In the current summer series of runs, half of the runs were made at night under conditions where the temperatures were constantly falling, and half of the runs were made during the daytime with constantly rising temperatures. Artifact levels during the rising temperature experiments were larger than those during the falling temperature runs, but attempts to make any quantitative comparisons are complicated by other differences between the run conditions. For example, the daytime temperatures were higher than the nighttime temperatures.

The general dependence of the extent of artifact formation on the volatility of individual compounds is illustrated in Figure 1. In this figure, we have used the logarithm of the vapor pressure of the pure compound at 25 C as a measure of its volatility. All of the volatile PAH measured in this program except for quinoline are included in this plot of the median values of the artifact level versus volatility. Artifact levels for quinoline are lower than the correlation suggested by this plot, as might be expected because of the greater polarity of quinoline.

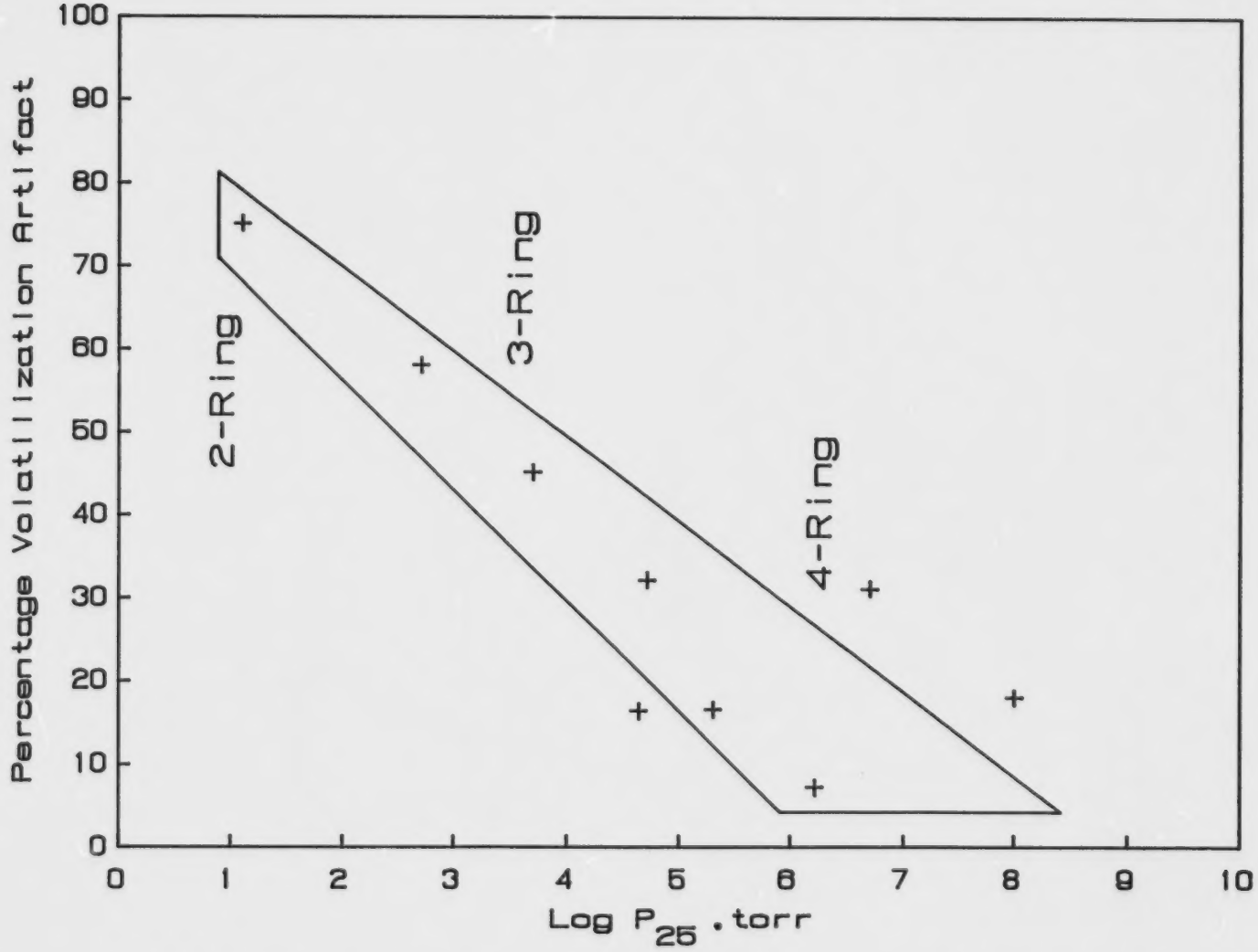

Figure 1. Dependence of Artifact Formation on PAH Volatility.

Adsorbed Phase

The total amounts of particulate matter collected in the current work ranged from about 30 $\mu g/m^3$ to about 150 $\mu g/m^3$, with the highest levels being found in the summer series and the lowest in the two indoor runs. The relative amounts of each of the volatile species (normalized with respect to phenanthrene) are shown in Figure 2. Considerable differences are seen between the distributions for the summer and winter data. In the case of naphthalene (offscale on winter plot), the relatively low values in the summer data are probably due to breakthrough of the PUF cartridge. However, no breakthrough is anticipated for the heavier PAH. It is possible that some of the low relative values in the summer experiments could reflect breakthrough of phenanthrene, but the constancy of the values for fluoranthene and anthracene argue against this. The lower values for acenaphthylene and pyrene in the summer study may be due to the reactivity of these compounds.

Although the total PAH composition appears to vary with the season, the normalized composition of the adsorbed phase is relatively constant. Examination of those data showed no consistent dependence on the sampling temperature. Figure 3 shows the means and standard deviations for the relative concentrations of the volatile PAH in the adsorbed phase.

Vapor Phase

In a stable parcel of air, the vapor phase and adsorbed phase are in local equilibrium, and consideration of the phase distribution must include the compositions of both phases. In our previous work (Coutant et al. 1988) it was shown that the Dubinin-Radushkevich (DR) isotherm was especially useful for describing the phase distribution of PAH in ambient air. This approach has been continued for the current data. In brief, the DR isotherm can be stated as

$$\ln (W/W_o) = B/b^2 [RT \ln P/P_o]^2$$

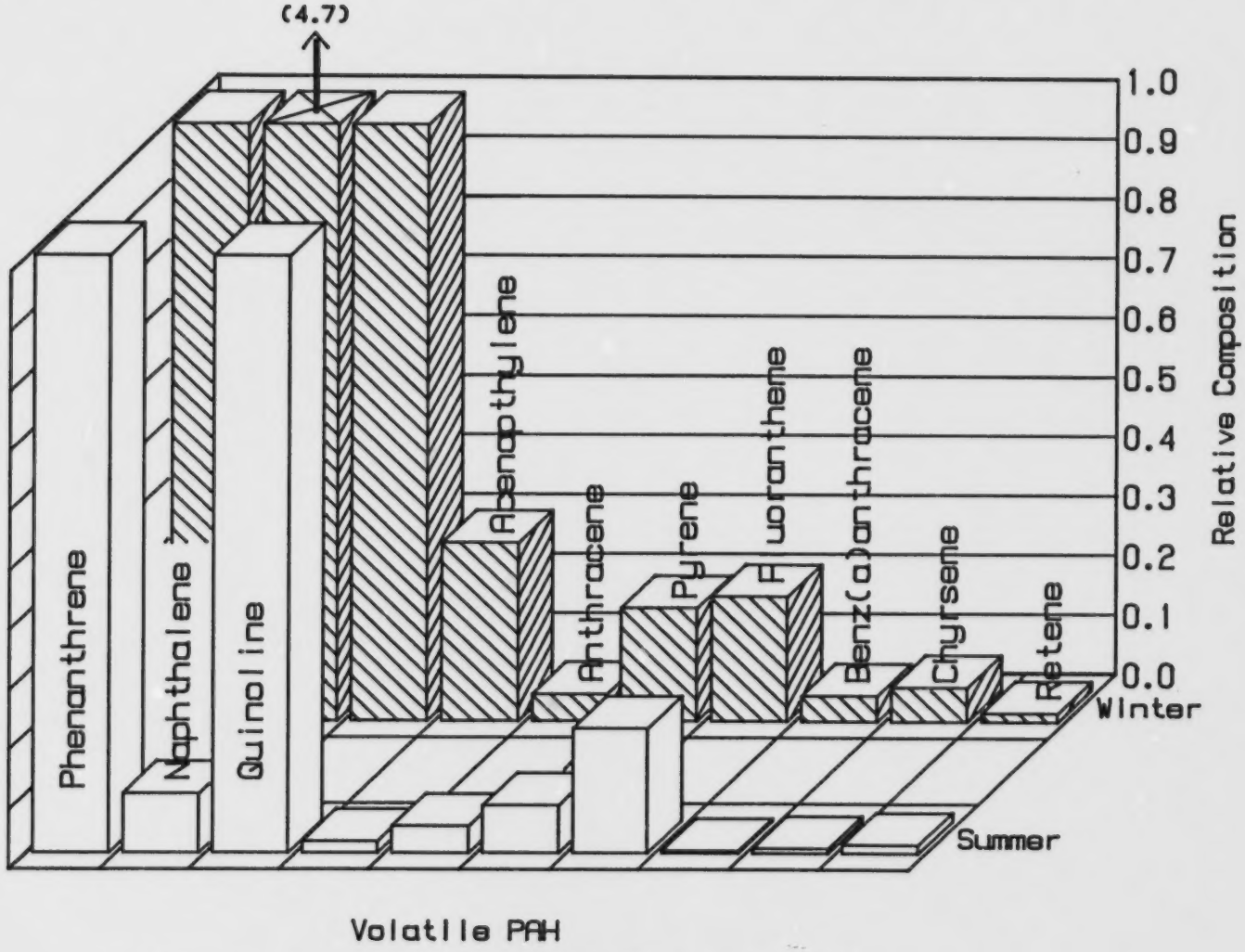

Figure 2. Composition of Volatile PAH in Total Sample.
(Normalized to Phenanthrene)

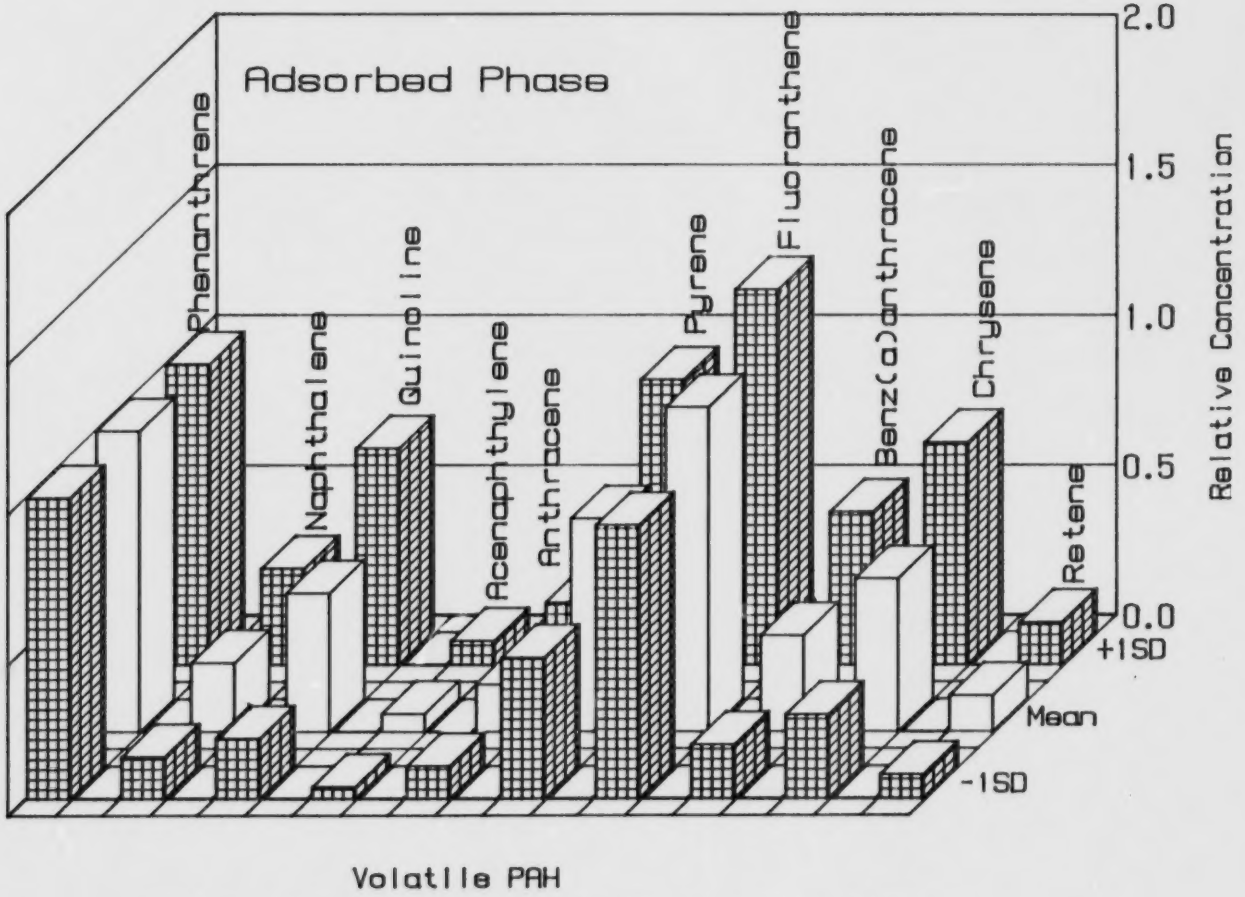

Figure 3. Composition of Volatile PAH in Adsorbed Phase. (Normalized to Phenanthrene)

where W is the adsorbed phase loading, W_o is the capacity of the sorbent, B is a constant that is characteristic of the sorbent, b is a function of the polarizability of the sorbate, P is the vapor phase concentration, and P_o is the equilibrium vapor concentration for the pure compound. The term in brackets is the isosteric heat of adsorption, which has units of energy/mole. When applied to mixtures of sorbates, as is the case with ambient PAH samples, the usual practice is to correct values of P_o for the relative composition of the mixture. However, because of the relatively constant composition of the adsorbed phase (see Figure 3), we have taken the approach of using P_o values of the pure compounds. In this case, the different values of W_o that are derived for various compounds reflect the relative compositions of those compounds in the adsorbed phase.

Figures 4-10 show DR plots for the volatile PAH. These plots include both the previous data and the current data where possible. Table 4 summarizes the DR parameters derived from these plots. Naphthalene, acenaphthylene, and quinoline were omitted from this table because of the limited number of data that were considered sufficiently accurate.

Table 4. Preliminary Dubinin-Radushkevich Parameters

Chemical	ln W_o	Slope B/b^2	M = Molar Refractivity		B = slope*M^2
Phenanthrene	5.00	0.061	62		234
Anthracene	3.30	0.051	64		209
Fluoranthene	4.80	0.074	68		342
Pyrene	4.40	0.066	68		305
Benz(a)anthracene	3.26	0.068	78		414
Chrysene	3.00	0.12	78		(730)
Retene	2.00	0.054	83		372
				Mean	313 ± 80

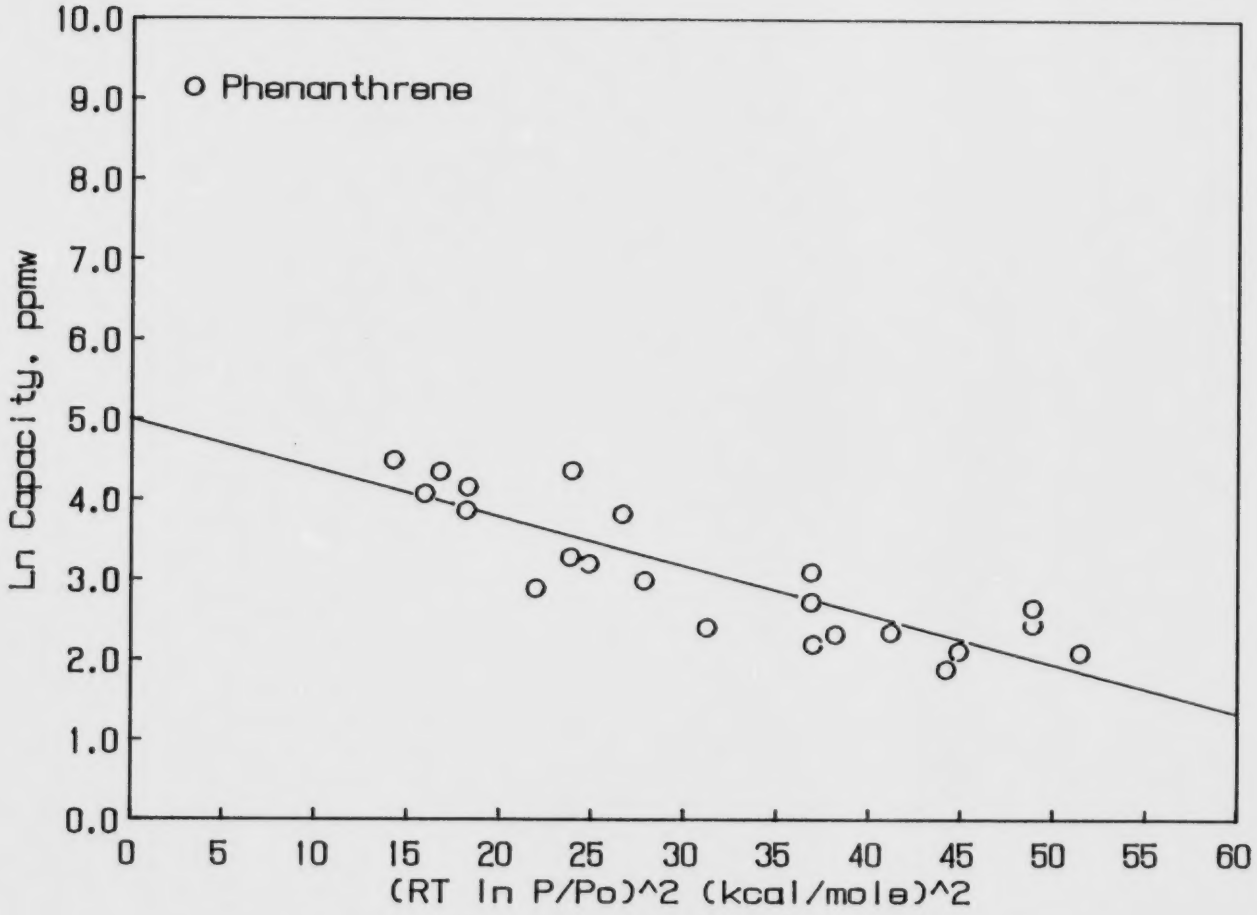

Figure 4. Dubinin-Radushkevich Plot for Phenanthrene.

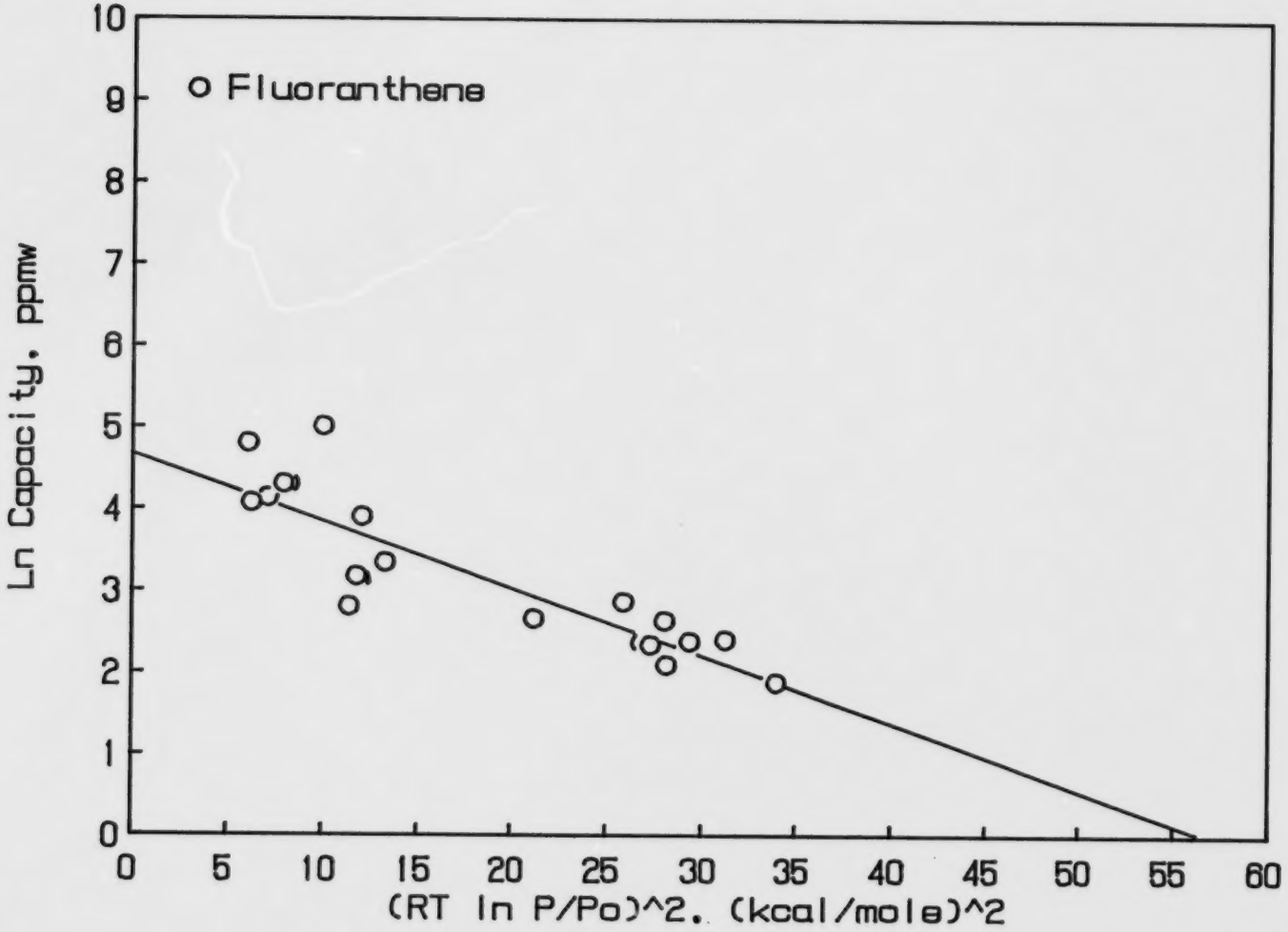

Figure 5. Dubinin-Radushkevich Plot for Fluoranthene.

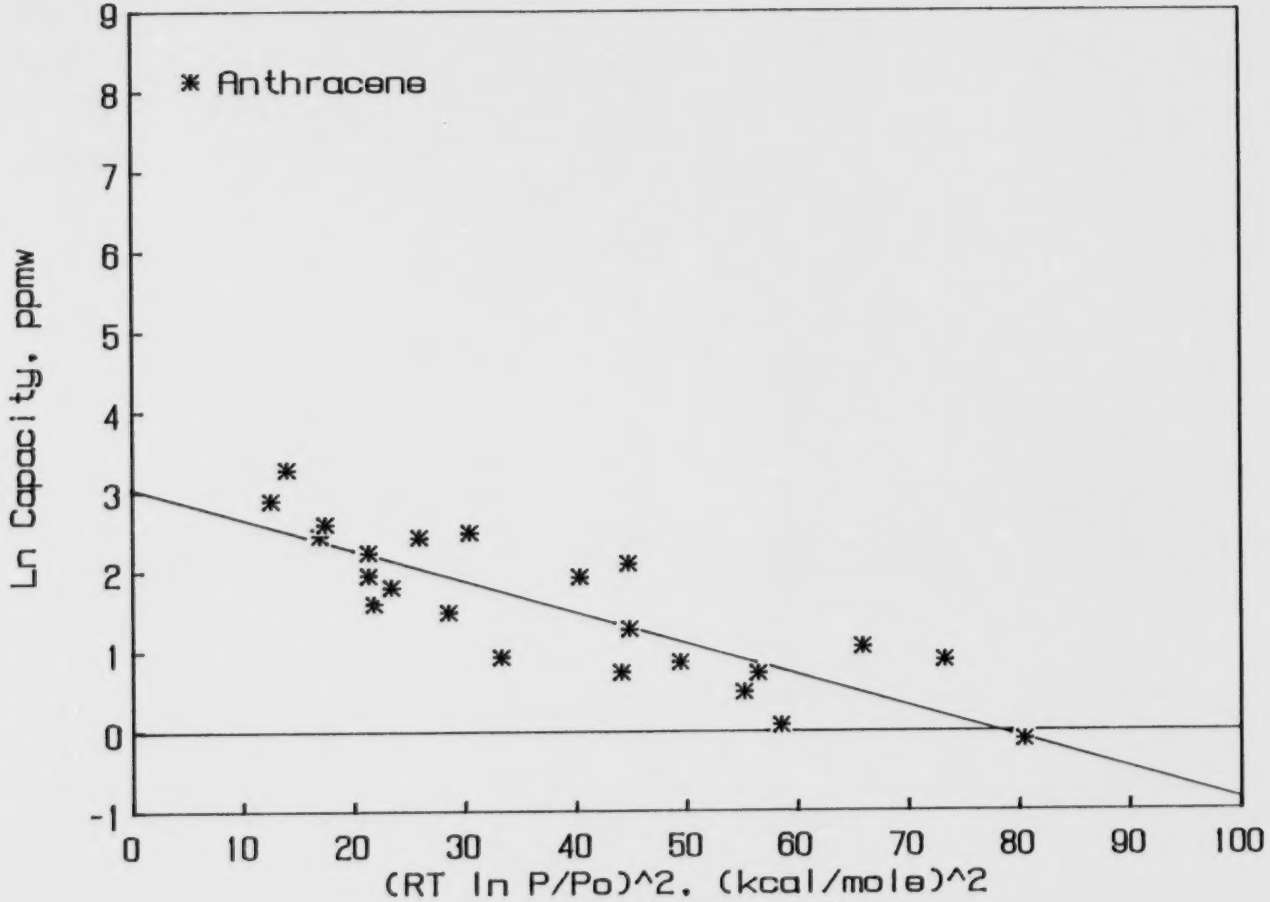

Figure 6. Dubinin-Radushkevich Plot for Anthracene.

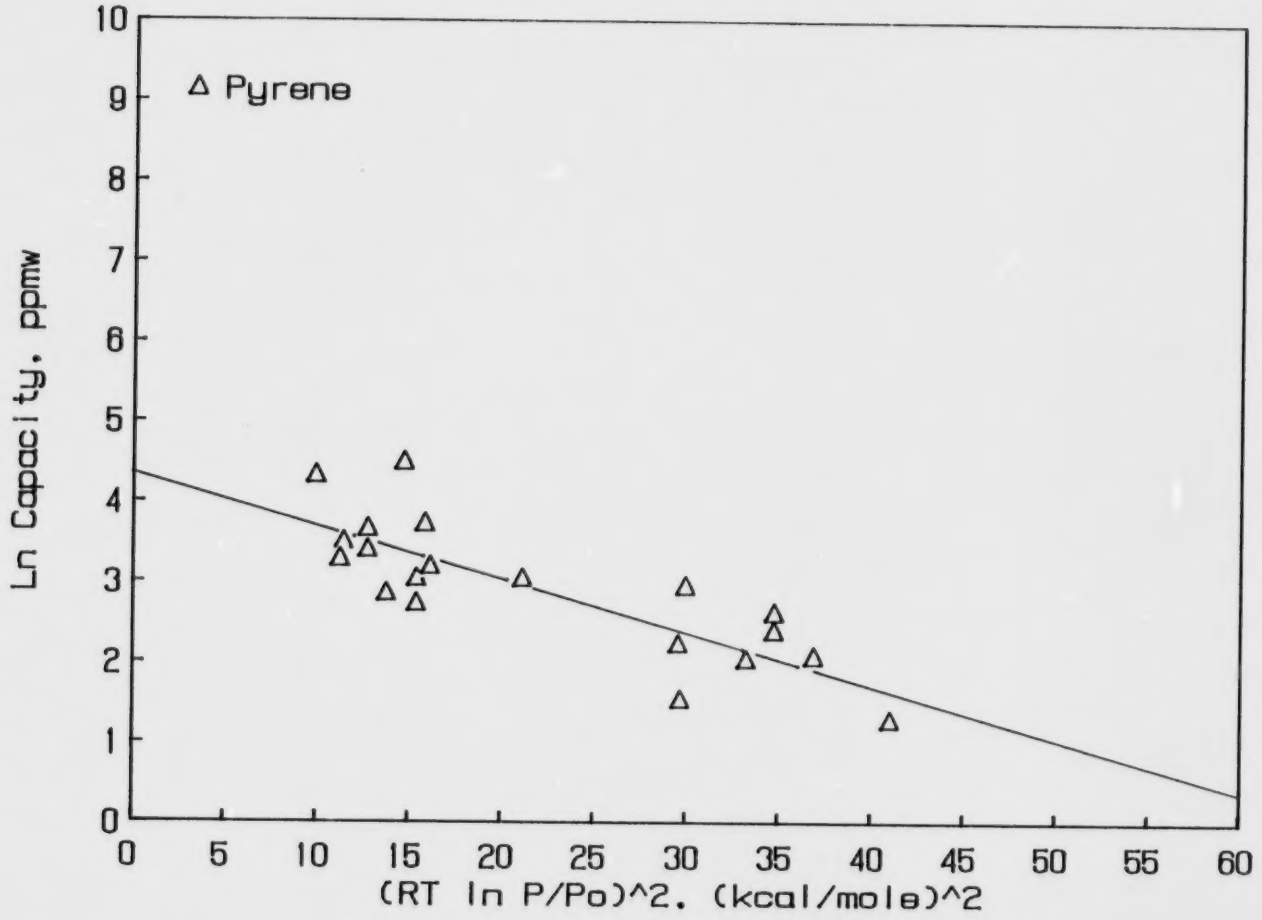

Figure 7. Dubinin-Radushkevich Plot for Pyrene.

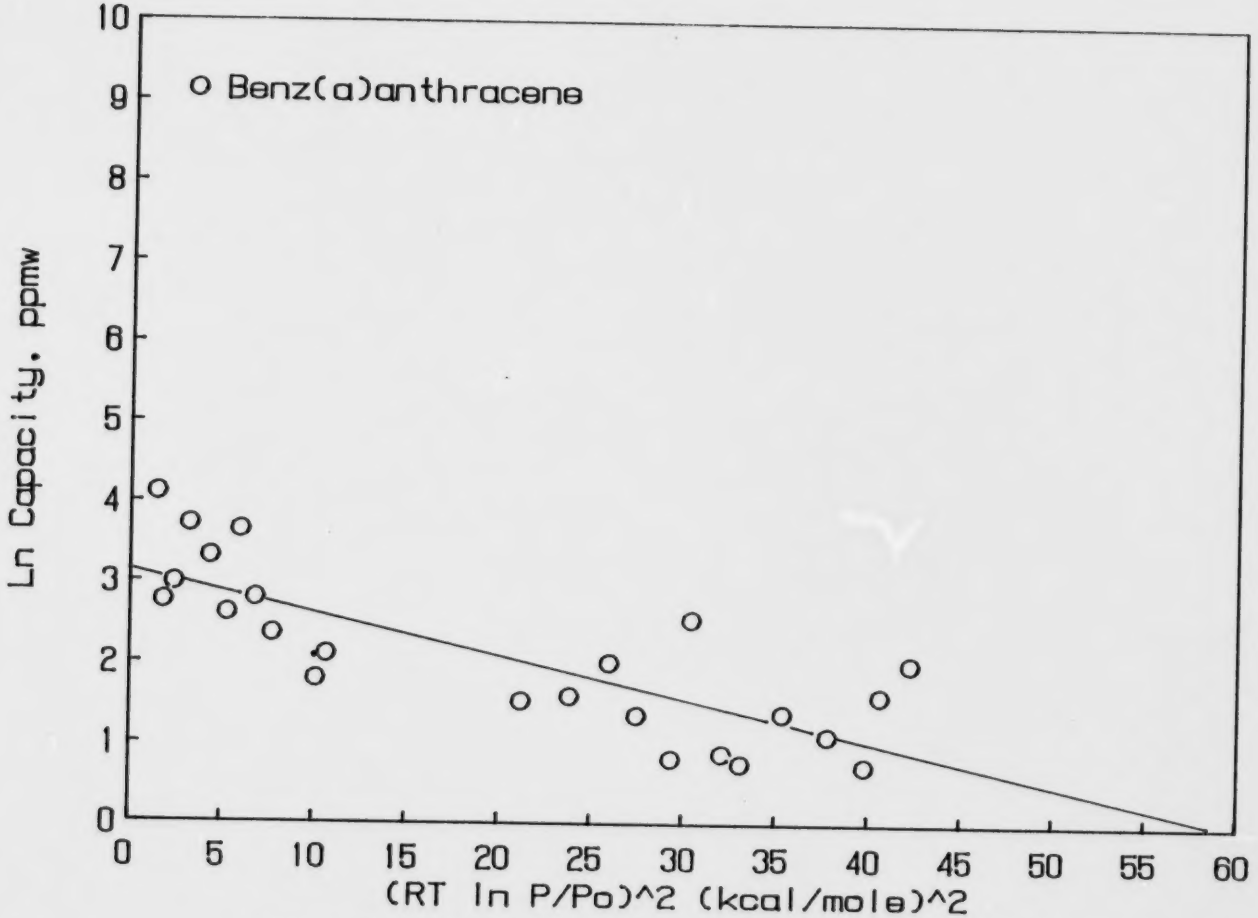

Figure 8. Dubinin-Radushkevich Plot for Benz(a)anthracene.

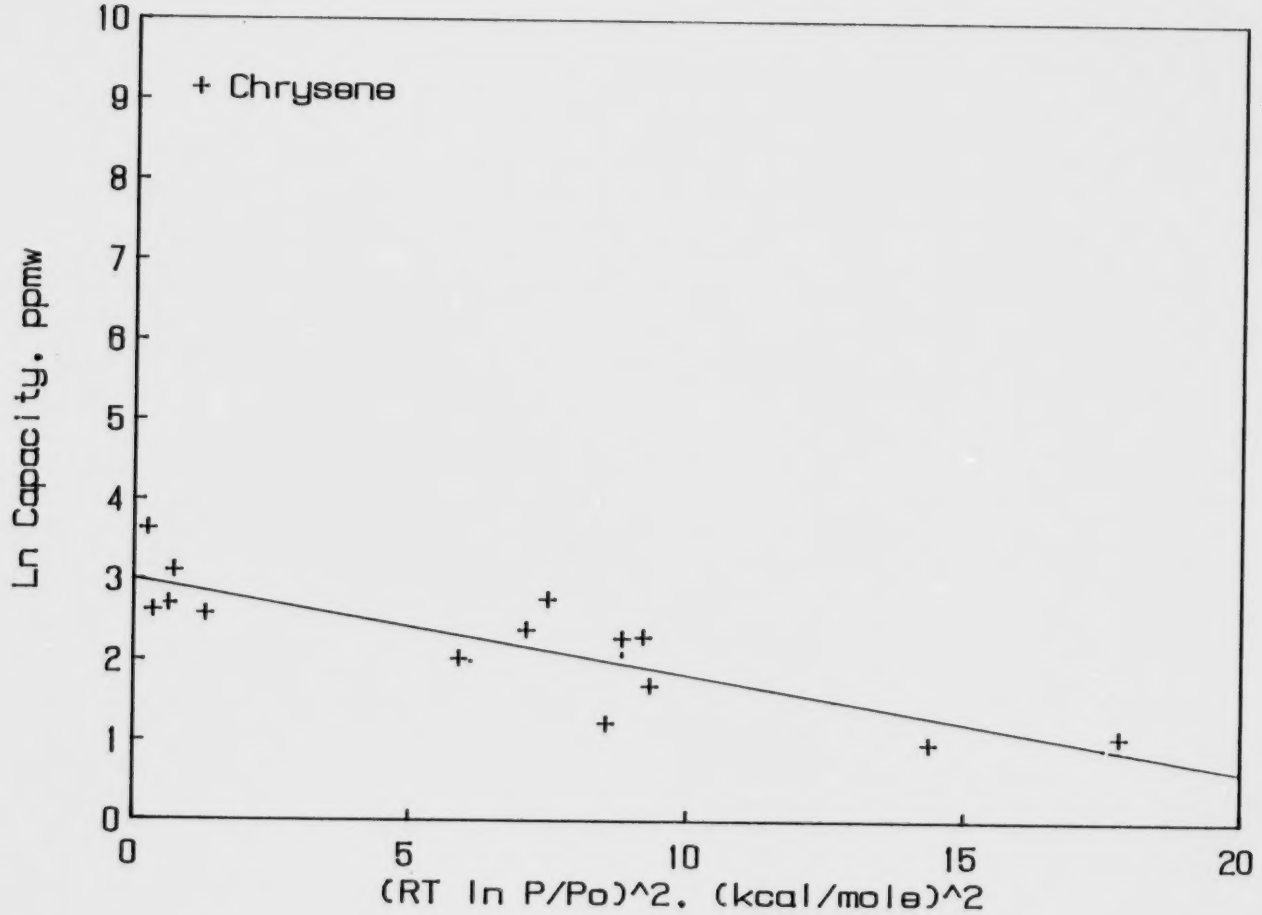

Figure 9. Dubinin-Radushkevich Plot for Chrysene.

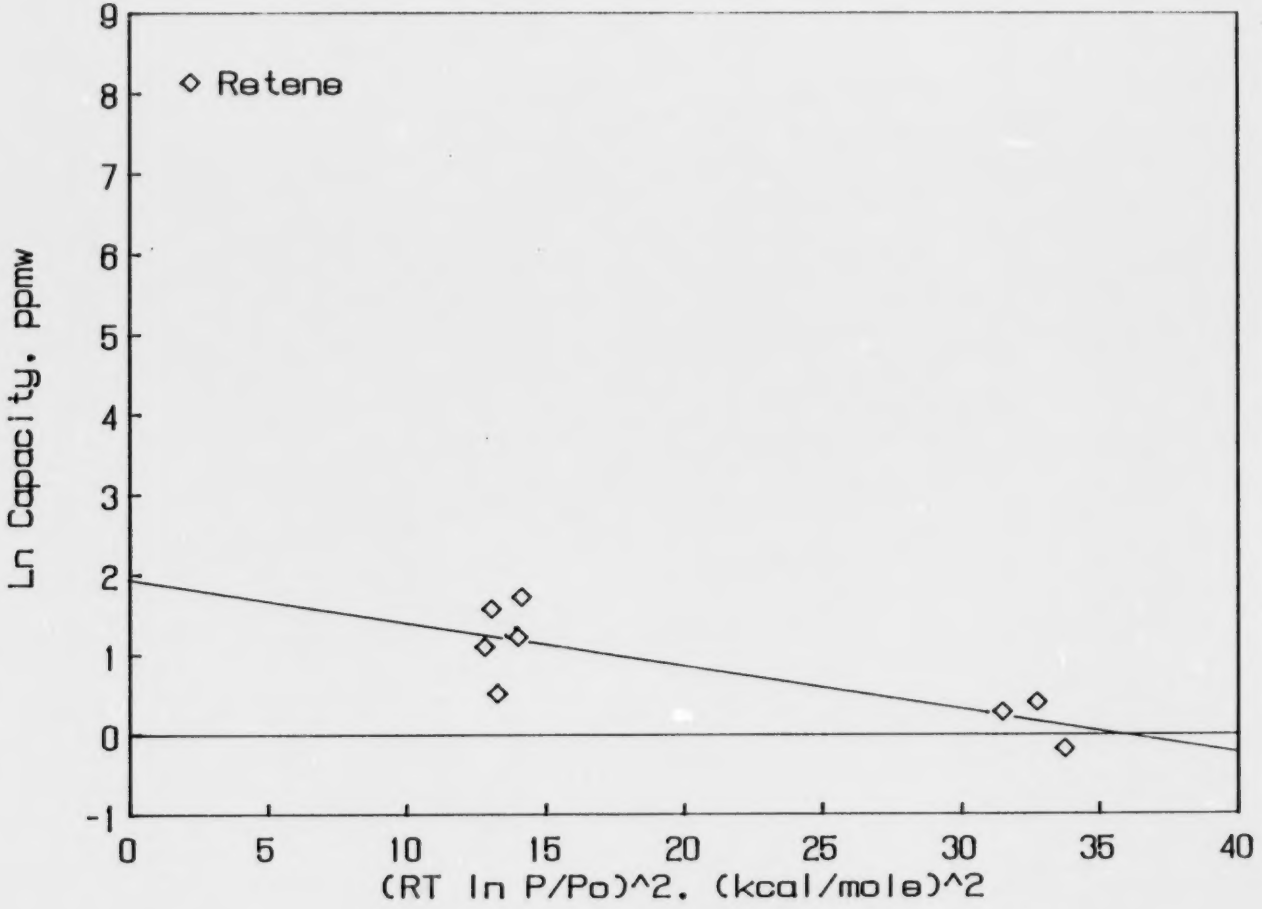

Figure 10. Dubinin-Radushkevich Plot for Retene.

In this table, the molar refractivities of phenanthrene and anthracene are based on literature values of their refractive indices; molar refractivities of the other compounds were estimated using standard group additivity techniques. In previous discussions we (Coutant et al. 1987) and others (Jonas et al. 1983) have shown that the parameter b in the DR equation is proportional to the molar refractivity of the sorbate. The product of the square of the molar refractivity and the slope of the DR plot should therefore be constant. In the current case, the mean value of B is 313 ± 25 percent. In an attempt to smooth out some of the scatter of the individual DR plots, and to better accommodate the limited range of variables for some of the compounds, the data for the seven compounds shown in Table 4 were combined using the mean value of B and variable offsets based on the centers of gravity for the data for each compound. The result is shown in Figure 11. It can be seen from this plot that the data for these seven compounds can be represented by a single slope. The only exception may be chrysene for which some of the data at very low values of P/P_o are displaced well above the mean curve. Those data however were close to the analytical limit, and may be subject to considerable error. Recommended DR parameters derived from this analysis are given in Table 5.

Table 5. Recommended Dubinin-Radushkevich Parameters

Chemical	ln W_o	M, Molar Refractivity	B	SD(a)
Phenanthrene	5.61	62	313	0.62
Anthracene	4.65	64	313	0.72
Fluoranthene	4.40	68	313	0.72
Pyrene	4.38	68	313	0.48
Benz(a)anthracene	3.10	78	313	0.75
Chrysene	2.55	78	313	0.51
Retene	1.76	83	313	0.36
			Mean	0.59

(a) Root mean square deviation between observed and calculated values of ln W.

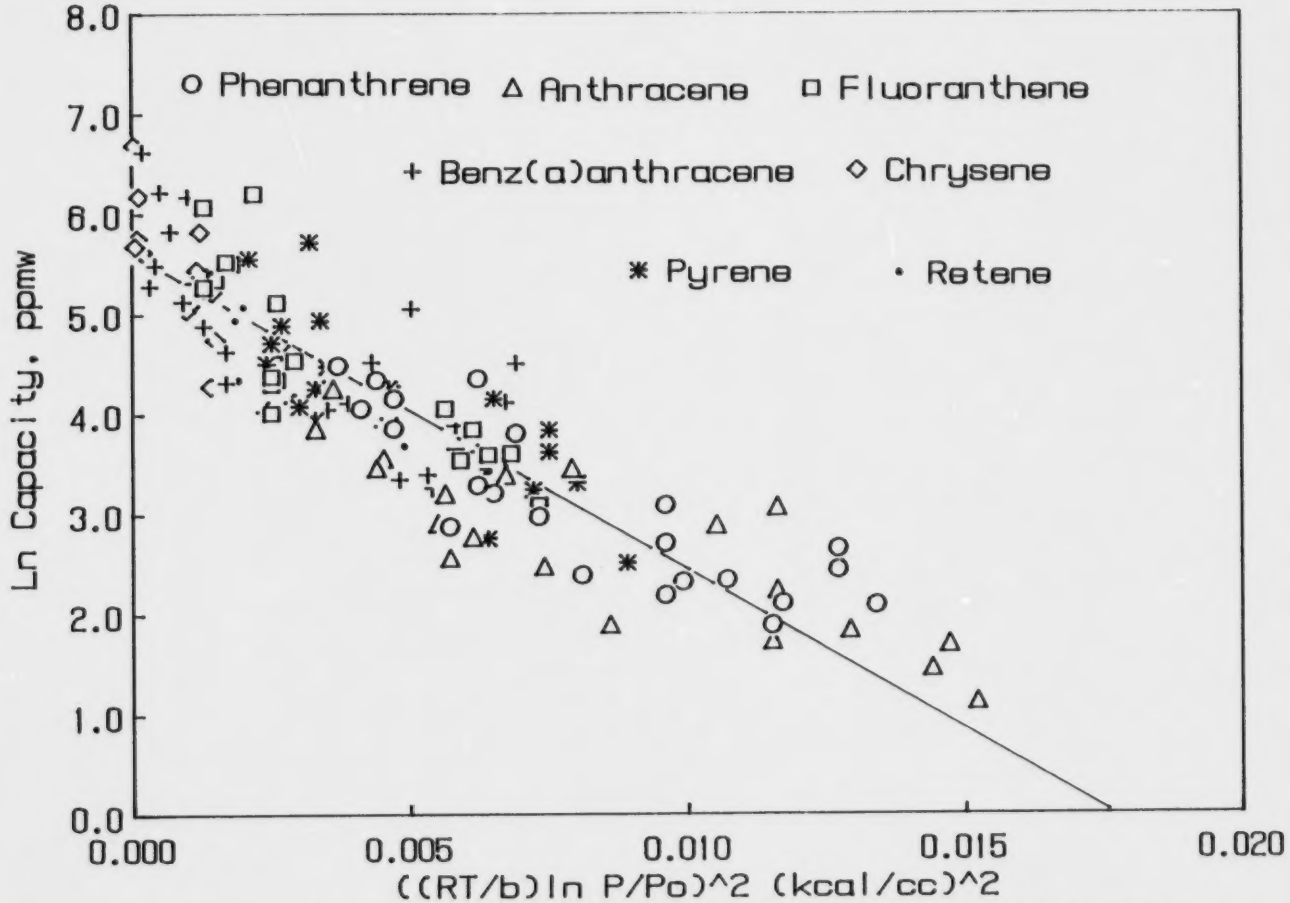

Figure 11. Generalized Dubinin-Radushkevich Plot for Volatile PAH.

Also given in this table are the standard deviations between the observed and calculated values of the logarithm of the capacity.

Generalizations

While there is considerable scatter in both the artifact and vapor phase data, this is not unexpected for experiments conducted under the uncontrolled conditions of normal ambient sampling. Nonetheless, the data display self-consistent trends that can serve as a basis for some generalizations concerning the phase distribution of PAH in ambient air. Figure 1 shows that the tendency for artifact formation is roughly proportional to the logarithm of the pure compound vapor pressure. A very approximate relationship derived from that data is

$$A(\%) = 76 - 8.7*\log(P_{25}) \qquad (\pm 15\%)$$

It should be noted that this relationship does not apply for quinoline or possibly other polar SVOC.

A similar generalization can be derived for the vapor phase concentrations of the PAH by considering Figure 12. This figure shows the band of measured vapor concentrations (log scale) plotted versus the logarithm of the pure compound vapor pressure. This figure illustrates the fact that the process of adsorption of PAH on ambient particulate matter lowers the equilibrium vapor pressure by an average factor of 14,000 (4,000 - 50,000) depending on ambient conditions and particulate loading. Thus, as a rule-of-thumb, we can expect ambient vapor concentrations of PAH to be 1/10,000 th of the pure compound vapor concentrations. Note that this does not exclude the heavier PAH such as BaP from being present in the vapor phase. Rather, their expected vapor concentrations are below the detection limits of commonly used sampling and analytical procedures.

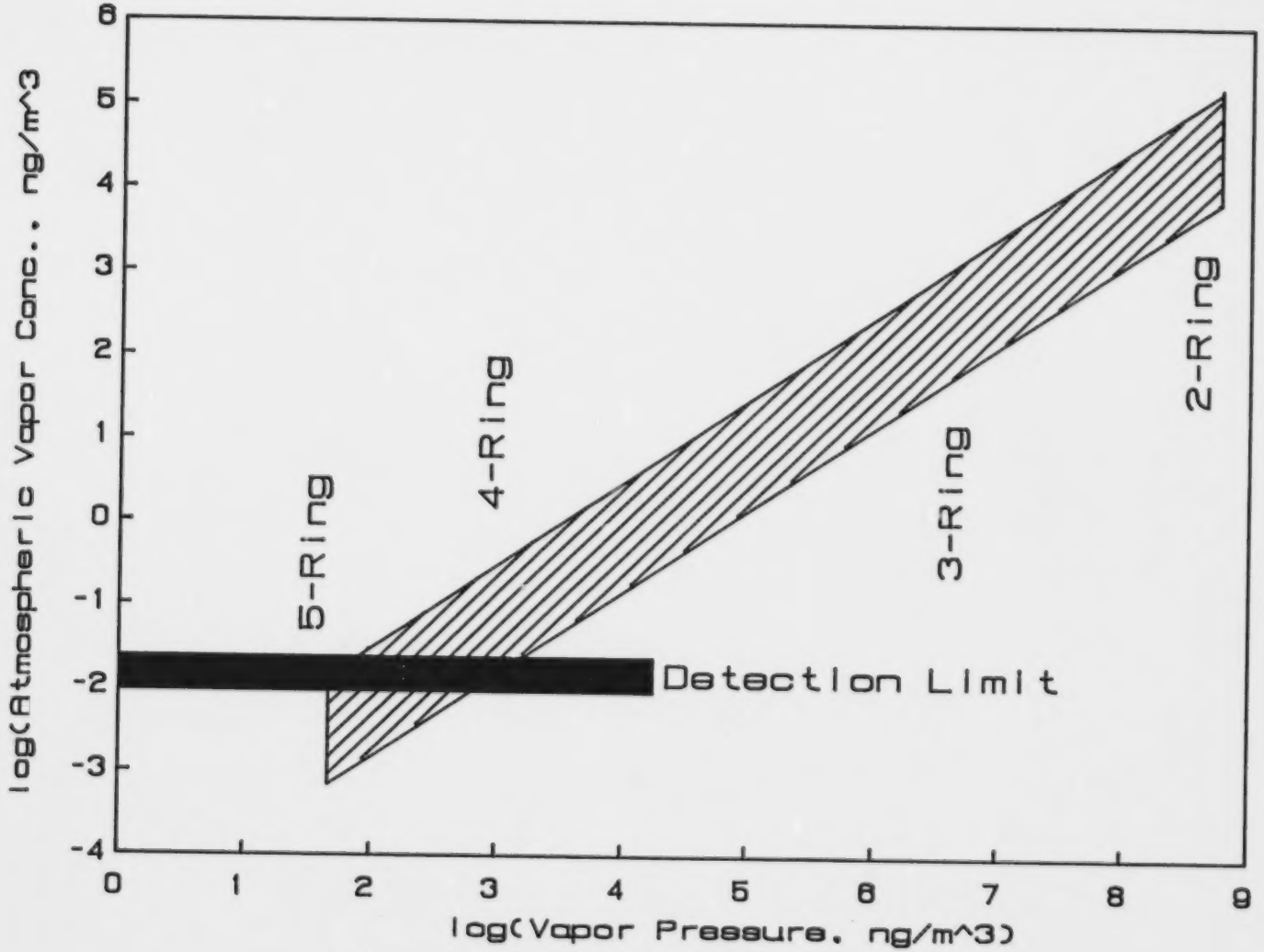

Figure 12. Generalized PAH Vapor Concentrations.

REFERENCES

1. Junge, C. E. "Fate of Pollutants in the Air and Water Environments--In Advances in Environmental Science and Technology (edited by Suffet, I. H.), Vol. 8 Wiley-Interscience, New York, 1977.

2. Yamasaki, H., Kuwata, K., and Miyamoto, H., "Effects of Ambient Temperature on Aspects of Airborne Polycyclic Aromatic Hydrocarbons", Envir. Sci. Technol., 16, 189 (1982).

3. Van Vaeck, L., Van Cauwenberghe, K., and Janssens, J., "The Gas-Particle Distribution of Organic Aerosol Constituents: Measurement of the Volatilization Artifact in Hi-Vol Cascade Impactor Sampling", Atmos. Environ., 18, 417-430 (1984).

4. Lane, A. L., Johnson, N. D., Barton, S. C., Thomas, G. H. S., and Schroeder, W. H., "Development and Evaluation of a Novel Gas and Particle Sampler for Semivolatile Chlorinated Organic Compounds in Ambient Air", Envir. Sci. Technol., 22, 941-947 (1988).

5. Coutant, R. W., Brown, L., Chuang, J. C., and Lewis, R. G., "Phase Distribution and Artifact Formation in Ambient Air Sampling for Polynuclear Aromatic Hydrocarbons", Atmos. Environ., 22, 403-409 (1988).

6. Fuller, E. N., Schettler, P. D., and Giddings, J. C., Ind. Eng. Chem., 58, 18 (1966).

7. Coutant, R. W., "Removal of Volatile Organics from Humidified Air by Adsorption", Final Report from Battelle Columbus Division to Environics Division Engineering & Services Lab, Tyndall Air Force Base, Contract No. F08635-85-C-01222, Sept. 15, 1987.

8. Jonas, L. A., Sansone, E. B., and Farris, T. S., Am. Ind. Hyg. Assoc. J., 44, 716-719 (1983).

APPENDIX A
Annular Denuder Design

(paper prepared for publication)

DESIGN AND PERFORMANCE OF A HIGH-VOLUME COMPOUND ANNULAR DENUDER

by

Robert W. Coutant*, Patrick J. Callahan, and Michael R. Kuhlman
Battelle Columbus Division
505 King Avenue, Columbus, Ohio 43201

and

Robert G. Lewis
U.S. Environmental Protection Agency
Research Triangle Park, North Carolina 27711

ABSTRACT

A laminar flow model incorporating variable collisional reaction efficiency is developed and applied for the design of annular denuders. Efficiencies predicted with the model show excellent agreement with published empirical data for annular denuders that are used for collection of SO_2, but point to potential errors in extending the empirical data to different chemical systems. The design and construction of a compound annular denuder for collection of polynuclear aromatic hydrocarbon vapor are described. This denuder, which consists of a nested set of cylindrical tubes, is shown to operate efficiently at sampling rates of up to 200 L/min, while maintaining essentially 100 percent transmission of micron-sized particulate matter.

INTRODUCTION

Diffusion scrubbers or denuders have been used for many years in a variety of applications related to sampling and analysis of ambient air pollutants. Most commonly they are used to remove selected vapor phase components from the sample stream while transmitting other vapor components and particles to subsequent stages of the sampling apparatus. Historically, most denuders have consisted of an open cylindrical tubular design, with design efficiency parameters being based on the equations of Gormley and Kennedy (GK)(1949). Examples of application of this type of design are found in Coutant et al.(1988) and Braman et al(1982). McMurry and Stolzenburg(1987),

and more recently Murphy and Fahey (1987), demonstrated a fundamental fault in the GK model in that the GK boundary condition is equivalent to the assumption of an infinite reaction rate at the denuder wall. A more realistic assumption is that the wall reaction rate is given by some fraction γ (the collision reaction efficiency) of the wall collision rate. Murphy and Fahey provide a mathematical model based on the approach of Cooney, Kim, and Davis (CKD)(1974) for calculating the effect of non-unitary γ in open cylindrical denuders.

Open cylindrical denuders are rapidly being replaced [Vossler et al.(1988) and Lane et al.(1988)] in many applications by annular denuders because of the greater efficiency of the annular denuders for a given size and flow condition [Possanzini(1983)]. Design of these annular denuders has thus far been based largely on the empirical relationship developed by Possanzini. CKD (1974) also presented an approach for calculating the efficiency of parallel plate denuders that should be applicable to annular denuders. However, the CKD approach has largely been ignored. This paper presents a design model for the annular denuder that includes the effect of non-unitary γ, and discusses results of application of this model to a compact nested or compound annular denuder. This new denuder is designed to be used with a conventional PS-1 sampler (Jackson and Lewis, 1982). It is distinguished by its ability to function efficiently at flow rates 10-20 times those currently used with single-stage annular denuders.

ANNULAR DENUDER MECHANICS

With typical annular denuders that are designed for high efficiency, the inner radius of the annulus is 90-95 percent of the outer radius, and the velocity distribution within the annulus is well-represented by the laminar flow equation for a thin planar slit [see Bird, Stewart and Lightfoot, 1960]. Reynolds numbers for these denuders are usually well below 2000 to ensure a laminar flow condition. Under such conditions, the problem of diffusive transport to the walls can be represented in terms of the parameters illustrated in Figure 1. Here, the x-coordinate is taken normal to the walls of the slit, with the origin along the centerline. B is the half-height of the slit,; the length of the slit in the direction of gas flow is L; and the width of the slit, W, is simply $\pi(r_1+r_2)$ where r_1, and r_2 are the bounding radii of

the annulus. For the case of a nested series of annular denuder, such as used by Lane et al, (1988), where the tubing sizes (o.d.) are consecutive multiples of the core diameter, d_o, it is convenient to note that the total effective slit width is given by:

$$W = \pi[nd_o + 2n^2B + n(n-1)T], \qquad (1)$$

where T is the wall thickness and n is the number of nested shells to be considered. Assuming that the flow velocity, v(x), is sufficient that diffusive transport is significant only in the x direction, and that the diffusing species is a minor constituent in the gas stream, the mass flux of the diffusing species at any point is given by:

$$J = -D\left(\frac{dC}{dx}\right) + Cv(x) \qquad (2)$$

where C is the local concentration and D is the diffusion coefficient.
Under steady-state conditions, the concentration distribution is given by the solution to the mass balance equation

$$D\left(\frac{\partial^2 C}{\partial x^2}\right) = \left(\frac{\partial}{\partial z}\right)(Cv(x)) \qquad (3)$$

For laminar flow through a planar slit, the velocity distribution is given by

$$v(x) = \frac{3V}{2}\left[1 - \left(\frac{x}{B}\right)^2\right], \qquad (4)$$

where V is the average velocity, which can be expressed as the bulk volumetric flow rate divided by the cross-sectional area (Q/2BW). Equation 3 thus becomes

$$D\left(\frac{\partial^2 C}{\partial x^2}\right) = \left(\frac{3Q}{4BW}\right)\left[1 - \left(\frac{x}{B}\right)^2\right]\left(\frac{\partial C}{\partial z}\right) \qquad (5)$$

Transforming the variables to non-dimensional form by letting:

$$X = x/B;\ C' = C/C_o;\ \text{and}\ Z = 4DWz/3QB$$

equation 5 reduces to

$$\left(\frac{1}{1-X^2}\right)\left(\frac{\partial^2 C'}{\partial X^2}\right) = \left(\frac{\partial C'}{\partial Z}\right) \tag{6}$$

With appropriate boundary conditions, equation 6 can readily be solved using the Crank-Nicolson finite-element method [see Crank, 1956].

Equations based on the assumption of zero concentration of the diffusing species at the wall, such as the GK equation, have proven useful for estimating denuder performance in many cases, but are physically unrealistic and can lead to significant errors. The proper boundary condition at the denuder wall is one that can account for the effect of finite reaction kinetics on the concentration gradient near the wall. The reactive flux, J_r, at the wall is given simply by:

$$J_r = -\gamma\left(\frac{Cu}{4}\right)_w \tag{7}$$

where u is the mean molecular velocity, and the diffusive flux to the wall, J_w, is

$$J_w = -D\left(\frac{dC}{dx}\right)_w \tag{8}$$

At steady state, these fluxes must be equal, and the gradient at the boundary is

$$\left(\frac{\partial C}{\partial x}\right)_w = \gamma\left(\frac{Cu}{4D}\right)_w \tag{9}$$

Murphy and Fahey(1987) suggest replacing γ by $\gamma/(1-0.5\gamma)$. This function reduces to γ at values less than about 0.1, and, as will be shown below, the consequences of finite reaction kinetics are not significant in practical denuder systems except at values of γ lower than about 0.005. Therefore, we prefer the simpler form of equation 9. For the other boundary conditions, C' = 1 at Z = 0, and there is a plane of symmetry at X = 0.

Collision Efficiencies

One problem with inclusion of γ in the computation of denuder efficiencies is that independently measured values of γ are rarely available, and γ can often only be inferred from comparison of the computational results to measured denuder efficiencies. Some guidelines are therefore needed for estimation of γ during denuder design, but experimentally derived values should ultimately be incorporated into representation of denuder performance.

Numerous citations of reaction efficiencies appear in the general body of literature dealing with such topics as condensation and evaporation, the kinetics of catalytic reactions, and heterogeneous reactions in the atmosphere. Values of γ reported for various reactions range from 1 to $<10^{-6}$. Except in a limited number of cases the reactions considered do not apply directly to cases of interest to denuder applications, but they can help to place limits on γ. Mortensen and Eyring (1960) have viewed the kinetics of gas adsorption in terms of an activated state consisting of a mobile two-dimensional layer. For reactions requiring essentially zero enthalpy of activation, the entropy of activation becomes the rate limiting factor. In this context, the loss of one degree of translational entropy or restriction of the rotational entropy suggests γ values in the range of 10^{-3} to 10^{-2} for non-linear polyatomic molecules. Alternatively, enthalpies of activation of just a few kcal/mole would yield values of γ in the same range. Condensation and evaporation (at clean surfaces under vacuum) of monatomic species such as metal vapors or rare gases are characterized by γ values in the range of 0.2 - 1 (McCarroll, 1964). The collision efficiency for condensation of water has been determined by Hickman (1954) to be in the range of 1×10^{-3} to 4×10^{-2}. Baldwin and Golden (1979) determined the collision efficiencies for several environmentally significant reactions, including the reaction of ammonia with

sulfuric acid, to be in the range of 10^{-4} to 10^{-3}. Recently, Lee and Tang (1988) determined that γ for the reaction of NO_2 with water is 6×10^{-4}. A further restriction on the value of γ is the condition of the reactive surface. Murphy and Fahey (1987) showed that surface contamination lowered the apparent reaction efficiency for NO_2 on gold from 8×10^{-3} to 8×10^{-4}.

In general, reactions having collision efficiencies less than about 5×10^{-5} are probably too slow to be considered within the constraints of practical denuder design for most applications. A few reactions, notably condensation processes and some acid-base reactions involving small molecules have collision efficiencies of the order of 10^{-3} or greater. Most other reactions that are known to be fast enough to be of some utility are likely to have γ values in the range of 5×10^{-5} to 10^{-3}. Based on the admittedly limited information in the literature, we recommend values close to 10^{-3} for reactions of small inorganic species and $2\text{-}5 \times 10^{-4}$ for sorption of large organic species as trial values for the collision efficiency in initial design calculations.

Denuder Design

Calculations of denuder efficiency based on equations 6 and 9 were performed using code written in C for IBM and compatible microcomputers with math co-processors. The code is menu oriented, allowing the user to rapidly explore different designs. Temperature and pressure dependent variables such as the diffusion coefficient and the Reynolds number are automatically corrected if the user changes these state variables. The diffusion coefficient is taken to be proportional to $T^{1.75}/P$ after the empirical correlation of Fuller, Schettler and Giddings (1966), and the Reynolds number is proportional to $P/T^{1.75}$.

Typically, the computation for a test set of variables is completed in 10-12 seconds (on a Compaq 286). Output is available in either tabular or graphical form as illustrated in Figure 2. In this figure, calculated values of the average concentration are plotted as a function of the non-dimensional ratio DWL/QB. Numbers at the right-hand ends of the curves are the values of the non-dimensional ratio $\gamma Bu/D$. The latter ratio results from expressing the boundary condition in non-dimensional terms.

The lowest curve in Figure 2 represents the limiting case of $\gamma = 1$ for the particular combination of variables used in this illustration. While exact values of u/D depend on temperature, pressure, and the molecular weight of the analyte, the overall magnitude of the ratio $\gamma Bu/D$ is determined largely by the value of the collision efficiency. In general, values of u/D are of the order of 3×10^3 cm^{-1}. Values of $\gamma Bu/D > 10^2$ generally yield denuder efficiencies that are approaching the diffusion-limited case. Therefore, the limiting value of γ for which the effects of finite reaction kinetics are significant is given approximately by

$$\gamma < \sim 3 \times 10^{-4}/B \qquad (10)$$

This relationship is similar to that derived by McMurry and Stolzenburg (1987) for open tubular denuders and it emphasizes the fact that annular denuders are more sensitive to the wall reaction rates than open tubular denuders simply because of the smaller gap size. For values of $\gamma < \sim 3 \times 10^{-4}/B$, the rate of analyte removal is in transition between the diffusion and chemical kinetics limits. For many annular denuders currently in use, B is of the order of 0.1 cm, so that for the removal process to be mainly diffusion limited, γ must be greater than about 3×10^{-3}. This is consistent with the findings of Murphy and Fahey (1987).

Table I shows a comparison of calculated efficiencies with the empirical results of Possanzini et al (1983). In this case, γ was varied until agreement was obtained with one arbitrarily selected experimental result and the same γ (0.0012) was then used for computation of the remaining cases. Note in Figure 2 that both the efficiency and the "intercept" change with γ, and that significant error could occur if Possanzini's empirical equation were applied to a system having a different γ. The calculated intercept for pure diffusion limited kinetics in an annular denuder is 0.75, whereas the curve for the case of pure wall reaction kinetics is a straight line (on a semi-log plot) passing through $C/C_o = 1$.

EXPERIMENTAL SECTION

One objective of this work was to develop an annular denuder system that would function efficiently for collection of phase-distributed polynuclear aromatic hydrocarbons (PAH) and other semivolatile organic compounds at sampling rates of 100 to 200 L/min while being sufficiently compact to be used with the PS-1 sampler. Empirical results (Coutant et al. 1988) with open tubular denuders coated with silicone grease for PAH sampling at low flow rates yielded reasonably good vapor collection efficiencies and capacities, but did not provide a means for extrapolation to the use of an annular denuder at the target flow rates. Experiments were therefore conducted using simple annular denuders similar to Possanzini's at linear velocities comparable to the target rates to gain estimates of both the thickness of absorptive coating needed for useful capacities and the collisional reaction efficiency for use in design calculations for the high-volume annular denuder (HVCAD). Naphthalene was used as a surrogate for PAH in these experiments.

Absorptive Coatings

Several different coatings were examined including high-vacuum silicone grease, a silicone pump oil, common grade SE-30,and GC-grade SE-30 (Alltech Associates). Several methods of application of the coatings were examined; the most generally useful and reliable method consisted of repeated immersion of the tubes in solutions of the stationary phase in dichloromethane. After drying, each tube was weighed to determine the average thickness of its coating, and additional coats of the stationary phase were then applied as necessary to provide essentially the same coating thickness on each tube. In attempting to apply SE-30 to the aluminum surface, it was necessary to pretreat the aluminum with a silanizing agent to obtain good wetting of the surface by the silicone. Coating thicknesses used ranged from 4 to 100 μm.

Efficiency and Capacity

Measurements of denuder efficiency and capacity for different coatings and coating thicknesses were made using naphthalene as the challenge

PAH. To perform these measurements, air containing naphthalene was passed through single shell annular denuders over a range of linear velocities typical of practical denuder use. Concentrations at the denuder inlet and outlet were monitored by gas chromatography (GC). Capacity was defined as the total amount of naphthalene passed through the denuder up to the time of 10 percent breakthrough. Final tests of the HVCAD efficiency were conducted by operating a PS-1 equipped with the denuder at two different flow rates (100 and 200 L/min) in a room in which the air had been spiked with naphthalene. Again, the inlet and outlet air concentrations were monitored by GC to determine the efficiency.

Particle Penetration

Two series of measurements were made to determine the efficiency of transmission of ambient particulate matter by the HVCAD. In the first set of runs, ambient laboratory air was drawn through the denuder, which was mounted on a PS-1 sampler, at 100 L/min and 200 L/min. The particle concentrations and size distributions were monitored before and after the denuder using a Laser Aerosol Spectrometer (Model LAS-X manufactured by PMS, Inc., Boulder, Colorado). In the second set of runs, cigarette smoke was added to the laboratory air, and the sampler was operated at a flow rate of 200 L/min.

EXPERIMENTAL RESULTS AND DISCUSSION

Coatings

Because of the need for relatively thick coatings to achieve capacities sufficient for application to ambient sampling, the silicone oil was not as useful as either silicone grease or SE-30. No significant difference in initial performance was observed between the latter two materials, but the grease is considerably easier to apply and remove. Initial tests of the SE-30 suggested that denuders coated with this material could be subjected to thermal desorption and repeated use. However, we noted that the efficiency of these SE-30-coated denuders declined significantly with repeated use. Examination of the SE-30 surface using ESCA showed that the surface was gradually being

oxidized by exposure to air. Successive ESCA analyses of a sample of SE-30 indicated approximately 30 percent oxidation of the surface after exposure to clean air at room temperature for a period of 30 days. Examination of the silicone grease with ESCA showed no detectable oxidation of this material over a period of 1-2 days exposure to air. Because of the greater ease of applying this material, subsequent tests of the denuder were performed using freshly applied coatings of the silicone grease.

Capacity and Efficiency

Results of the measurements of efficiency and capacity are summarized in Table II. The results indicate that the capacity, as well as the efficiency, is a function of the linear velocity, and that the capacity is a function of the film thickness. Analysis of the limited data in Table II suggests that the capacity is exponentially dependent on linear velocity and linearly dependent on the film thickness, viz.:

$$\text{Cap}(\mu g/cm^2) = 0.003d\ e^{-0.0095V} \quad , \qquad (11)$$

where d is the film thickness in μm, V is the average linear velocity in cm/s, and the naphthalene capacity is given in $\mu g/cm^2$. Based on previous measurements of PAH vapor concentrations in ambient air (Coutant et al. 1988), we estimate that the total capacity required for 24-h sampling of ambient air at a sampling rate of 200 L/min is of the order of a few tens of micrograms.

For most of the runs cited in Table II, the initial effluent concentration was below the detection limits of the chromatograph being used, so that the efficiencies cited are lower limits. In the one case where the naphthalene was initially detectable, comparison with calculated performance suggests a γ of about 0.0003. This value was therefore used in initial design calculations for the HVCAD.

Denuder Design

Several different designs were considered based on use of commercially-available tubing sizes and wall thicknesses, using the model cited

above to provide guidelines. The most economic use of space was achieved using a nested series of 12 annular denuders as shown in Figure 3. For the current purpose, this high-volume compound annular denuder (HVCAD) was constructed using commercially available aluminum tubing, 1.6 mm (1/16 in) wall thickness, in diameter increments of 6.4 mm (0.25 in). The core is 6.4 mm aluminum rod, and the spacings between the tubes are maintained by three-armed radial rake assemblies that are attached to the core. The rake assembly at one end is held in place by a wing nut for easy disassembly and cleaning or coating of the tubes. The overall length of the HVCAD is 20.32 cm (8.0 in), and the outer diameter is 8.25 cm (3.25 in). In use, the HVCAD is mounted within a close-fitting aluminum shell that is equipped with O-ring-sealed end caps. This shell serves both as a protective transport container and, with the end caps removed, as an interface with the PS-1 filter holder.

With this denuder, the calculated efficiency of collection of an "average" semivolatile PAH (M = 178 g/mole; D = 0.062cm^2/sec; γ = 0.0003) is 94.9 percent at a sampling rate of 100 L/min. Results of the full scale laboratory test using naphthalene as the challenge vapor indicated a slightly better performance, with an apparent value of γ of 0.0004. Application of equation 9 to the case of the HVCAD at 200 L/min (velocity = 130 cm/s; area = 6600 cm^2) suggests a capacity of about 6 μg/μm of surface coating. Because of the tentative nature of equation 9, coating thicknesses used with the HVCAD were increased to a minimum 30 μm to provide a margin of safety.

Particle Penetration

Results of the two series of particle penetration measurements made with the HVCAD are shown in Figures 4 and 5. Although there appear to be some small discrepancies between the particle size distributions measured before and after the denuder, it should be noted that these distributions were measured sequentially rather than simultaneously. The differences between the observed curves are typical of the normal range of variation in particle size distribution found in the laboratory, and no measurable particle removal can be attributed to the denuder. Indeed, because of the relatively small diffusivities of particles, we would not expect to see any significant trapping of ambient aerosol by the denuder as long as laminar flow is maintained and

there are no significant impingement effects at the inlet [see, for example, DeMarcus and Thomas (1964)].

CONCLUSIONS

Results of this work illustrate the importance of the collisional reaction efficiency in both design and use of annular denuders. The model has proven useful for both design and applications purposes. Copies of the source code and/or a compiled version can be obtained by sending a blank diskette to the principal author (RWC). The compound annular denuder that was designed using the model developed in this work is capable of efficient collection of PAH vapor at sampling rates up 200 L/min, while maintaining essentially 100 percent transmission of ambient particulate matter.

DISCLAIMER

Although the work described in this article was funded in part by the U.S. Environmental Protection Agency through Contract No. 68-02-4127, it has not been subjected to Agency review. It, therefore, does not necessarily reflect the views of the Agency, and no official endorsement should be inferred. Mention of trade names or commercial products does not constitute endorsement or recommendation.

LITERATURE CITED

Baldwin, A. C. and Golden, D. M. (1979) Heterogeneous Atmospheric Reactions: Sulfuric Acid Aerosols as Tropospheric Sinks. *Science*, 206, 562-563.

Braman, R. S.; Shelley, T. J.; McClenney, W. A. (1982) Tungsten VI Oxide for Preconcentration and Determination of Gaseous and Particulate Ammonia and Nitric Acid in Ambient Air. *Anal. Chem.*, 54, 358-364.

Bird, R. B.; Stewart, W. E.; Lightfoot, E. N. (1960) *Transport Phenomena*, John Wiley & Sons, Inc., New York, 51-63.

Cooney, D. O.; Kim, S. Davis, E. (1974) Analyses of Mass Transfer in Hemodialyzers for Laminar Blood Flow and Homogeneous Dialysate. *Chem. Eng. Sci.*, 29, 1731-1738.

Coutant, R. W.; Lewis, R. G.; Chuang, J.; Brown, L.; Riggin, R. (1987) Phase Distribution and Artifact Formation in Ambient Air Sampling for Polynuclear Aromatic Hydrocarbons. *Atmos. Environ.*, 1988, 22, 403-409.

Crank, J. (1956) *The Mathematics of Diffusion*, Oxford University Press, Chapter 10.

DeMarcus, W. and Thomas, J., U.S. AEC Report ORNL-1413 (1952) as found in Fuchs, N. A., *The Mechanics of Aerosols*, C. N. Davies (Ed.), The MacMillan Co., New York, 1964, 206.

Fuller, E. N.; Schettler, P. D.; Giddings, J. C. (1966) A New Method for Prediction of Binary Gas-Phase Diffusion Coefficients. *Ind. Eng. Chem.*, 58, 18-27.

Gormley, P. G. and Kennedy, M. (1949) Diffusion from a Stream Flowing through a Cylindrical Tube. *Proc. R. Ir. Acad.*, 52A, 163-169.

Hickman, K. C. D. and Torpey, W. A. (1954) Evaporation of Resting Water. *Ind. Eng. Chem.*, 46, 1446-1450.

Lane, A. L., Johnson, N. D.; Barton, S. C.; Thomas, G. H. S.; Schroeder, W. H. (1988) Development and Evaluation of a Novel Gas and Particle Sampler for Semivolatile Chlorinated Organic Compounds in Ambient Air. *Envir. Sci. Technol.*, 22, 941-947.

Lee, J. H. and Tang, I. N. (1988) Accommodation Coefficient of Gaseous NO_2 on Water Surfaces. *Atmos. Environ.*, 22, 1147-1151.

Lewis, R. J. and Jackson, M. D. (1982) Modification and Evaluation of a High-Volume Air Sampler for Pesticides and Semivolatile Industrial Organic Chemicals. *Anal. Chem.*, 54, 592-594.

McCarroll, B. and Ehrlich, G. (1964) Condensation and Energy Transfer on Crystals in *Condensation and Evaporation of Solids* ed. E. Rutner, P. Goldfinger, and J. P. Hirth, Gordon and Breach Science Publishers, New York, 526-527.

McMurry, P. H. and Stolzenburg, M. R. (1987) Mass Accommodation Coefficients from Penetration Measurements in Laminar Tube Flow. *Atmos. Environ.*, 21, 1231-1234.

Mortensen, E. M. and Eyring, H. (1960) Transmission Coefficients for Evaporation and Condensation. *J. Phys. Chem.*, 64, 846-849.

Murphy, D. M. and Fahey, D. W. (1987) Mathematical Treatment of the Wall Loss of a Trace Species in Denuder and Catalytic Converter Tubes. *Anal. Chem.*, 59, 2753-2759.

Possanzini, M.; Febo, A.; Liberti, A. (1983) New Design of a High-Performance Denuder for the Sampling of Atmospheric Pollutants. *Atmos. Environ.*, 1983, 17, 2605-2610.

Vossler, T. L.; Stevens, R. K.; Paur, R. J.; Baumgardner, R. E.; Bell, J. P. Evaluation of Improved Inlets and Annular Denuder Systems to Measure Inorganic Air Pollutants. Accepted for publication in *Atmos. Environ.*, January 26, 1988.

Table I. Results of SO_2 Annular Denuder Simulation
(L=20 cm; B=0.8 mm; D=0.136 cm^2/sec; γ=0.0012)

Flow Rate, cm^3/s	Eff.,% (exp)	Eff.,% (cal)	Intercept(a)
83	98.7	98.7	0.836
97	98.0	97.6	0.836
113	96.5	96.1	0.835
125	94.8	94.8	0.829
147	92.5	92.2	0.829
175	88.5	88.7	0.828
198	85.0	85.9	0.828
225	82.4	82.5	0.828
238	81.3	81.0	0.828

(a) Curve extrapolated from log-linear portion of curve to L=0.

Table II. Summary of Denuder Efficiency and Capacity Measurements

Denuder Type(a)	Sorbent Coating	Velocity, cm/s	Film Thick., μm	Capacity, μg(b)	Efficiency percentage(c)
Glass	Si-grease	7.0	~100	99	>98
Glass	Si-grease	29.2	~100	32	>96
Glass	Si-grease	55.6	~100	60	>97
Glass	Si-grease	178.0	~100	>18	77
Aluminum	Si-grease	14.0	~80	68	>93
Aluminum	Si-grease	90.3	~80	30	>91
Aluminum	SE-30	14	3.5	4	>94
Aluminum	SE-30	14	14	19	>94

(a) L = 21.6 cm, W = 7.5 cm, B = 0.08 cm
(b) Total naphthalene removed at 10% breakthrough level
(c) Minimum initial removal efficiency; effluent naphthalene below detection limits for most runs

FIGURE CAPTIONS

1. Geometry used to represent thin annulus.

2. Effect of denuder dimensions, molecular properties, and flow rate on denuder performance.

3. Photograph of compound annular denuder with casing and end caps.

4. Laboratory air aerosol distributions measured with and without denuder in system.

5. Aerosol distributions measured with (o) and without (•) denuder in system using laboratory air plus cigarette smoke.

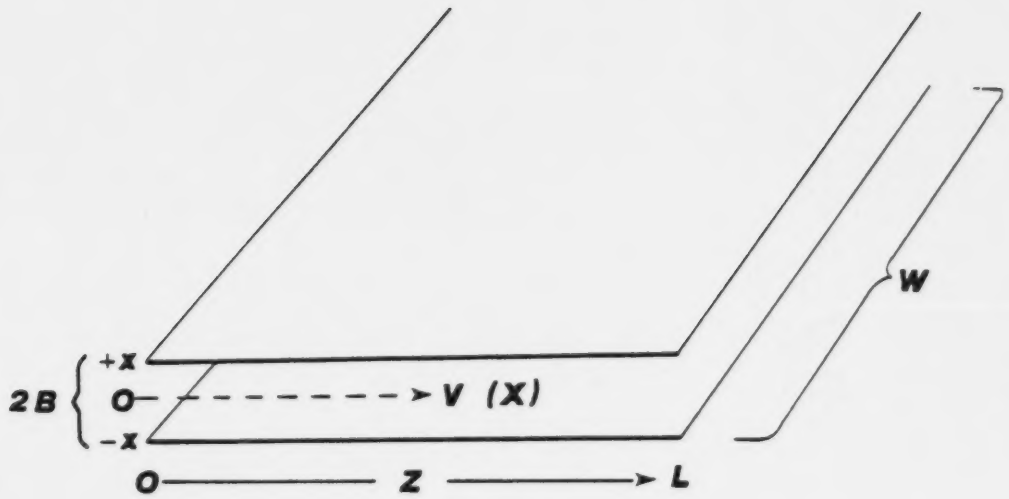
+x
2B
0
-x
V (X)
W
0
Z
L

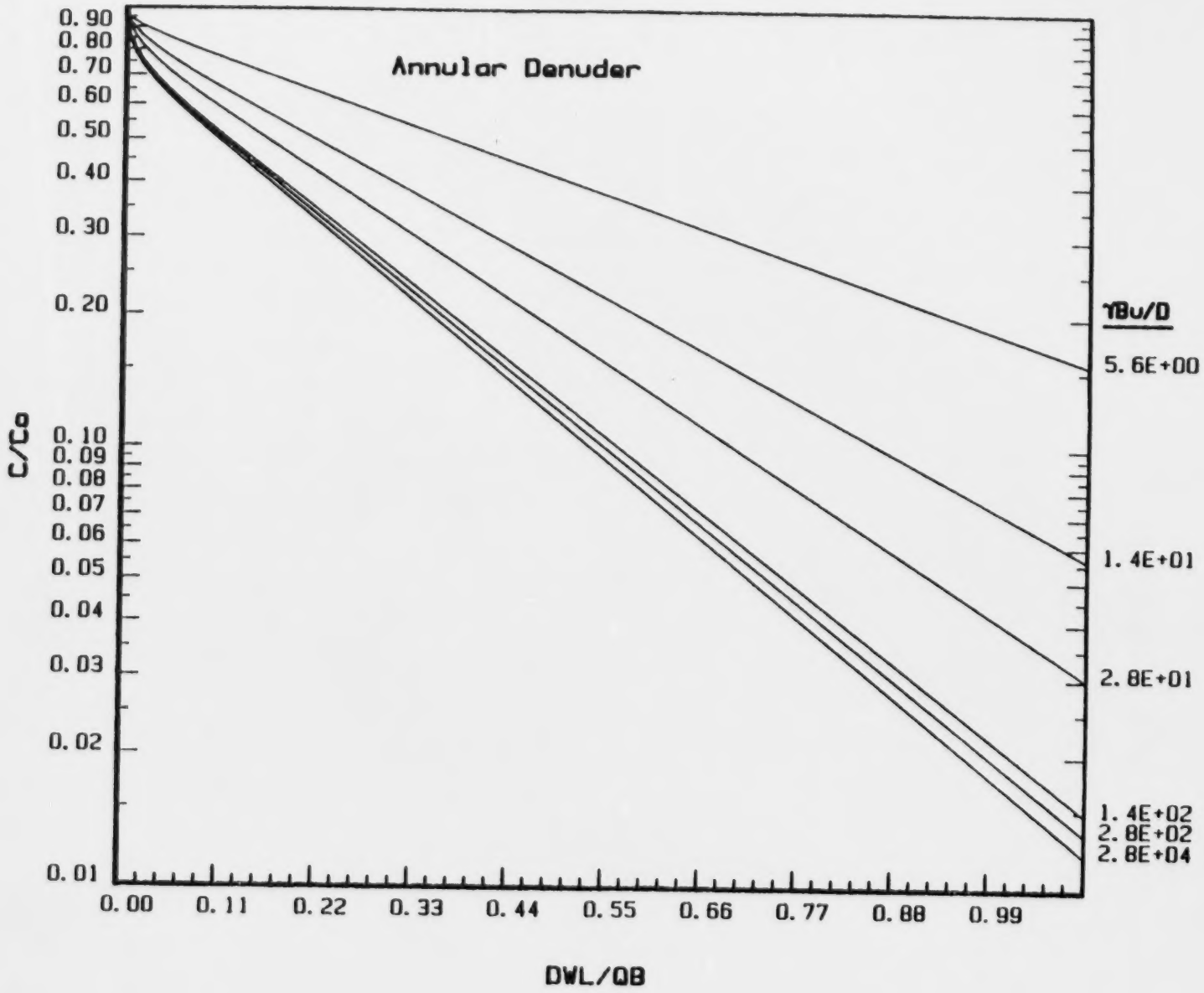
Annular Denuder
C/Co
0.90
0.80
0.70
0.60
0.50
0.40
0.30
0.20
0.10
0.09
0.08
0.07
0.06
0.05
0.04
0.03
0.02
0.01
0.00
0.11
0.22
0.33
0.44
0.55
0.66
0.77
0.88
0.99
DWL/QB
γBu/D
5.6E+00
1.4E+01
2.8E+01
1.4E+02
2.8E+02
2.8E+04

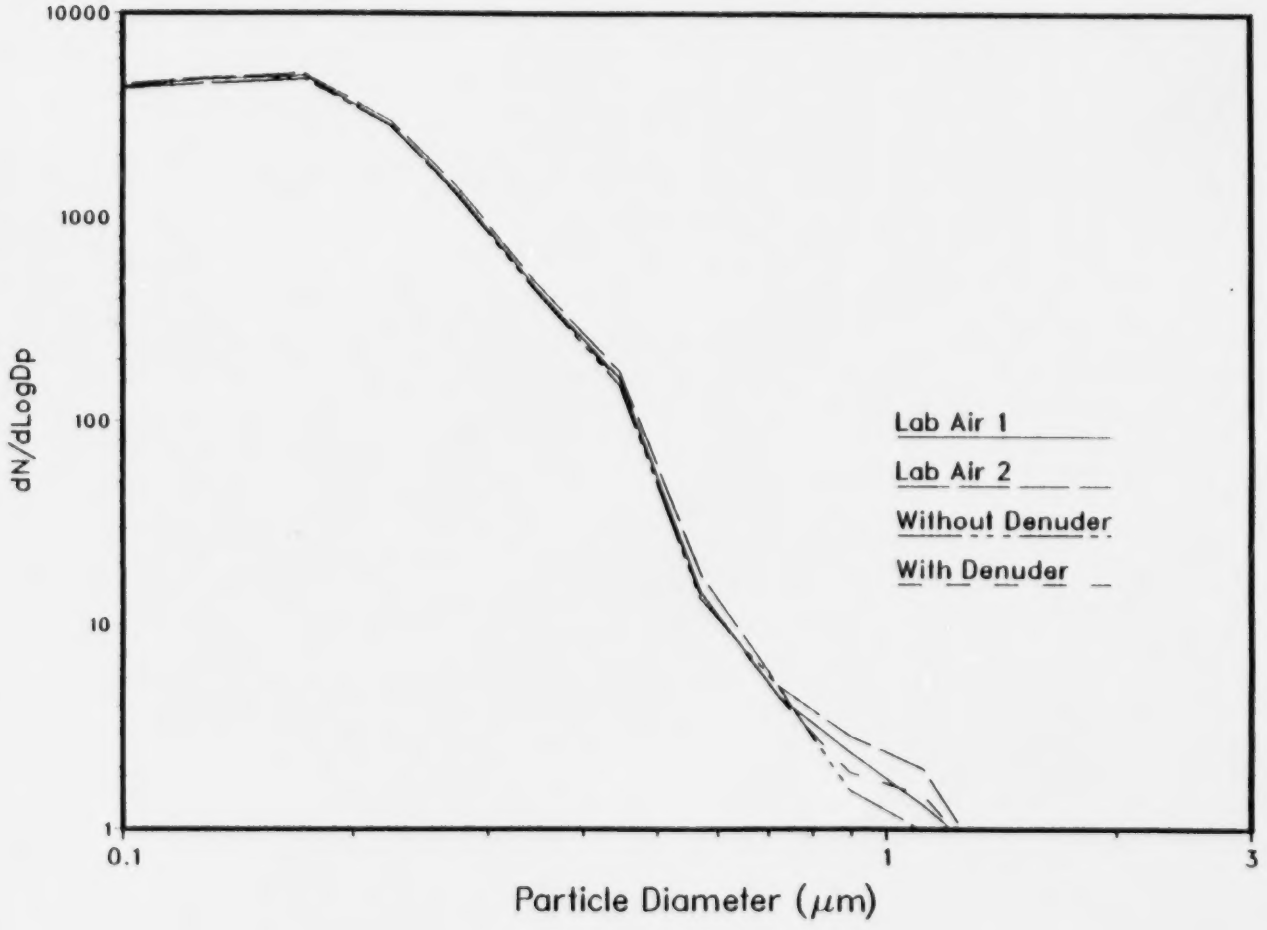
10000
1000
100
10
1
dN/dLogDp
0.1
1
3
Particle Diameter (μm)
Lab Air 1
Lab Air 2
Without Denuder
With Denuder

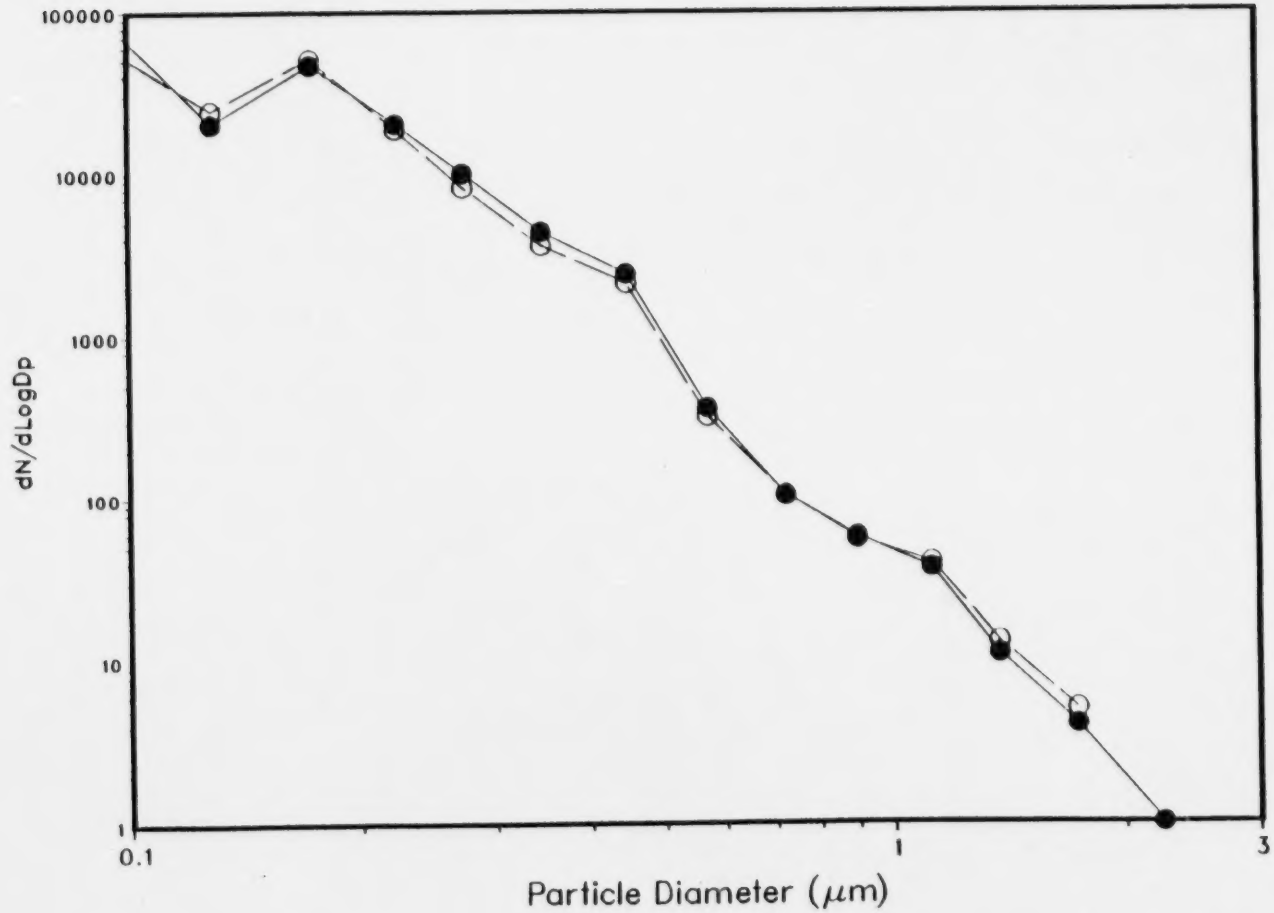
100000
10000
1000
100
10
1
dN/dLogDp
0.1
1
3
Particle Diameter (μm)

SOURCE CODE

A copy of the source code for the model developed on this program is not included in the paper for publication but is appended here as a part of this report.

The following is a printout of the source code for the computer program developed for simulation of annular denuder performance. This code was written using Microsoft C v5.0, which supports the proposed ANSI standard, but includes some language extensions. A compiled version of the code is available on request. This version of the code was written specifically for use with 80286/80287 machines, with EGA display. It supports hard copy output to a plotter that uses HPGL. The code uses the Crank-Nicolson method for solution of the differential equations.

```
#include <math.h>
#include <string.h>
#include <float.h>
#include <stdio.h>
#include <conio.h>
#include <graph.h>
#include <ctype.h>
#include <malloc.h>
#include <process.h>
#define COM1 0;
#define LPT1 0;
char far *buffer;
int BFL[8],i,jj,j,k,N,nd,dsn;int n=1;
float Q=166.67;float L=20;float D=0.136;float T=298.0;float M=64;
float B=0.08;float W=3.644;int ST=10;float STZ=200.0;float P=1.0;float wt;float
dO=1.0;
float alpha,beta,z;float E=0.0012;float
slope,in,NX,hx,hy,zz,yo,NRE,dy,xp,yp,yo1;
double c[50][5],tt,tlt,test;float cb[1000];float x[50];
char resp[2];FILE *stream;
char fname[15]; char res;char buf1[5];
char buf[90]; char pr='i';char ans;
```

```
int tm[640];int m[10];

main()

{

start:    for (i=0;i<=7;i++) BFL[i]=3;if(resp[0]=='e'){goto exit;}
     menu ();
     beta = (B*E*14551/(4*D))*sqrt(T/M);
matrix: N= STZ; NX =ST;
     _settextposition (16,25);_settextcolor (28);_outtext("      Working
");
     for (i=0;i<=ST+1;i++){ c[i][0]=1;}
     for (j=0;j<=N;j++){cb[j]=0;}
     jj=1;k=0;tlt=2.0;for (i=1;i<=ST;i++) {x[i]=(float)(1-i/NX);}
     z=STZ/(alpha*pow(NX,2));
comp:     tt=c[1][1];cb[0]=1;k=k+1;
     c[0][1]=c[1][1]*(1/(1+beta/NX));
     for (i=1;i<=ST;i++){
     if (BFL[1]==11) z=(STZ/(alpha*pow(NX,2)))*(1-pow(x[i],2));
     c[i][1]=c[i][0]*((z-1)/(1+z))+(.5/(1+z))*(c[i+1][0]+c[i+1][1]+
c[i-1][0]+c[i-1][1]); }
     c[ST+1][1]=c[ST-1][1];
     tt=fabs(tt-c[1][1]);if (tt >= 1e-08) goto comp;
     test=tlt/cb[jj-1];tlt=cb[jj-1];cb[jj]=0;
     for (i=0;i<=ST-1;i++){ cb[jj]=cb[jj]+.5*(c[i][1]+c[i+1][1]);}
     cb[jj]=cb[jj]/NX;
     test=fabs(test-tlt/cb[jj]);if (test <=1e-06) goto ave;
     jj=jj+1;for (i=0;i<=ST+1;i++) {c[i][0]=c[i][1];}
     k=0;if (jj<=N+2) goto comp;
ave: slope=log(cb[jj-1]/cb[jj-2]);in=cb[jj-1]*exp((1-jj)*slope);
     for (j=jj;j<=N+1;j++) {cb[j]=cb[j-1]*exp(slope);}
     if (BFL[5]==11){ store ();}
     if (BFL[4]==11){plot () ;}
     goto start;
exit:     _clearscreen(_GCLEARSCREEN);_setvideomode(_DEFAULTMODE);
```

```
}

menu ()
{
input:  _clearscreen (_GCLEARSCREEN); _setvideomode(_TEXTC80);
       _settextcolor (14);_settextposition (1,30);_outtext ("Annular
Denuder");_settextcolor(2);
     _settextposition(3,5);_outtext ("(F)low Rate = ");sprintf
(buf1,"%4.0f",Q/16.667);_outtext(buf1);_outtext (" L/min");
     _settextposition(3,50);_outtext ("(L)ength = ");sprintf
(buf1,"%3.1f",L);_outtext(buf1);_outtext (" cm\n");
     _settextposition(4,5);_outtext ("(D) = ");sprintf
(buf1,"%1.3f",D);_outtext(buf1);_outtext (" cm^2/sec");
     _settextposition(4,50);_outtext ("(T) = ");sprintf
(buf1,"%3.1f",T-273);_outtext(buf1);_outtext(" C");
     _settextposition(5,5);_outtext ("(M) = ");sprintf
(buf1,"%3.0f",M);_outtext(buf1);
     _settextposition(5,50);_outtext ("Slit (W)idth = ");sprintf
(buf1,"%4.1f",W);_outtext(buf1);
     _outtext (" cm\n");
     _settextposition(6,5);_outtext ("(C)ollision efficiency =
");sprintf(buf1,"%1.1e",E);_outtext(buf1);
     _settextposition(6,50);_outtext ("(G)ap = ");sprintf
(buf1,"%1.3f",B);_outtext(buf1);_outtext (" cm");
     _settextposition(7,5);_outtext("(P)ressure =
");sprintf(buf1,"%3.0f",P*760);_outtext(buf1);_outtext(" torr");
     _settextposition (8,5);_outtext("DWL/QB =
");sprintf(buf1,"%1.2f",D*W*L/(Q*B));_outtext (buf1);
      _settextposition(8,50);_outtext("(H)elp");_settextposition(7,50);_out-
text("Reynolds No. = ");
     NRE= Q*P*1.37e05/((W+2*B)*pow(T,1.75));if (NRE>=1000){_settextcolor(28);}
     sprintf(buf1,"%4.0f",NRE);_outtext(buf1);
     _settextposition (10,30);_settextcolor (14);_outtext ("Flow Type");
     _settextposition (11,20);_settextcolor (BFL[1]);_outtext ("(1) Laminar");
     _settextposition (11,40);_settextcolor (BFL[2]);_outtext ("(2) Plug
flow");_settextcolor (3);
```

```
     _settextcolor (14);_settextposition (13,30);_outtext ("Output Choices");
     _settextcolor (BFL[3]);_settextposition (14,10);
     if (pr=='i'){_outtext("(3) IBM Printer");}
     if (pr=='e'){_outtext("(3) Epson Printer");}
     _settextposition (14,30);_settextcolor (BFL[4]);_outtext("(4) Plotter");
     _settextposition (14,50);_settextcolor (BFL[5]);_outtext("(5) Disk");
     if((BFL[1]+BFL[2])==14){if((BFL[3]+BFL[4]+BFL[5])>=17){BFL[0]=11;
     _settextcolor (12);_settextposition(16,25);_outtext("(R)eady to
calculate");}}
     _settextcolor(3);_settextposition(18,5);
     _outtext("To change any of above parameters, type key letter or
number\n");
     while(!kbhit()); resp[0]=getch();resp[0]=tolower(resp[0]);
     switch (resp[0]){
     case 'h':
          help();
          break;
     case 'd':
          printf (" Input Diffusion coefficient at 25 C and 1 atm ");
          scanf ("%f",&D);
          D=D*pow((T/298),1.75)/P;
          break;
     case 't':
          printf ("Input temperature (C) ");
          D=D*pow((298/T),1.75);
          scanf ("%f",&T);T=T+273;
          D=D*pow((T/298),1.75);
          break;
     case 'p':
          printf ("Input pressure (torr) ");
          D=D*P;
          scanf ("%f",&P);P=P/760;D=D/P;
          break;
     case 'f':
          printf ("Input volumetric flow rate (L/min) ");
          scanf ("%f",&Q);Q=16.667*Q;
```

```
          break;
     case 'w':
          printf("%s\n\r","Do you know W or want to calculate it ? (K/C) ");
          while(!kbhit());ans=getch();ans=tolower(ans);switch(ans){
          case 'k':
               printf("Input W (cm) ");
               scanf("%f",&W);break;
          case 'c':
               printf("Input number of shells  ");
               scanf ("%d",&n);
               printf ("Input core diameter (cm) ");scanf("%f",&d0);
               if(n>1){printf ("Input shell wall thickness (cm)
");scanf("%f",&wt);}
               W=3.14159*(n*d0+2*B*pow(n,2)+n*(n-1)*wt);
               B=(0.5*d0-wt)/2;
               }
          break;
     case 'm':
          printf ("Input molecular weight  ");
          scanf ("%f",&M);
          break;
     case 'l':
          printf ("Input denuder axial length  ");
          scanf ("%f",&L);
          break;
     case 'g':
          printf ("Input annulus gap half-width  ");
          scanf ("%f",&B);
          break;

     case '1':
          BFL[2]=3;
          BFL[1]=14-BFL[1];
          alpha=(4*D*W*L)/(3*Q*B);
          break;
     case '2':
```

```
            BFL[2]=14-BFL[2];BFL[1]=3;
            alpha=(2*D*W*L)/(Q*B);
            break;
       case '3':
            BFL[3]=14-BFL[3];
            printf ("(I)BM or (E)pson printer ? ");
            scanf ("%s",&pr); pr=tolower(pr);
            break;
       case '4':
            BFL[4]=14-BFL[4];
            break;
       case '5':
            BFL[5]=14-BFL[5];
            printf ("(S)tore new data or (R)etrieve old data ?");
            while(!kbhit());res=getch();res=tolower(res);
            printf ("\n\r%s","Input file name ");
            scanf ("%s",fname);
            if (res=='r'){
            stream = fopen (fname, "r");
            fscanf
(stream,"%d\,%f\,%d\,%f\,%f\,%f\,%f\,%f\,%f\,%f\,%f\,%f\,%f",&ST,&STZ,&N,&L,&B,&W,-
&Q,&D,&T,&E,&M,&in);
            for (i=1;i<=7;i++){fscanf (stream,"%d",&BFL[i]);}
            for (i=0;i<=N+1;i++){fscanf (stream,"%f",&cb[i]);}
            fclose (stream);BFL[5]=14-BFL[5];
            plot();}
            break;
      case 'r':
            if(BFL[0]==3){_settextcolor(12);_settextposition(19,1);
            _outtext("Please complete selection of flow type and output mode
before starting");
            printf("\n\r%s","Press return to resume");
            while(!kbhit());break;}
            printf("%s %d %s %3.0f %s\n","Current model is ",ST," radial nodes by
",STZ," length nodes-- ok? (Y/N)");
            while(!kbhit());res=getch();res=tolower(res);if (res=='n'){
```

```
            printf ("Input # radial nodes  ");
            scanf ("%d",&ST);
            printf ("\nInput # length nodes  ");
            scanf ("%f",&STZ);}
            return (0);
      case 'c':
            printf ("Input Collisional Reaction Efficiency   ");
            scanf ("%f",&E);
            break;
      case 'e':
            break;
      default:
            printf ("Try again"); }
      goto input;
}

plot ()
{
      _clearscreen (_GCLEARSCREEN);
      _setvideomode (_ERESCOLOR) ;_setcolor(11);
      _moveto (0,3);
      _lineto (0,0);
      _moveto (0,3);
      _lineto (7,3);
      buffer =(char far *)malloc((unsigned int)
            _imagesize(0,0,10,10));
      _getimage(0,0,10,10,buffer);
      _clearscreen (_GCLEARSCREEN);
      _rectangle (_GBORDER,110,1,639,280);_settextcolor(14);
      _settextposition(23,40);_outtext("DWL/QB");
      _settextposition(10,2);_outtext("C/Co");
      _settextcolor(12);nd=fabs(log10(cb[N]))+1;yo=pow(10,-nd);
      for (j=1;j<=nd;j++){dy=yo*pow(10,j-1);
      for (yp=yo*pow(10,j-1);yp<=yo*pow(10,j);yp+=dy){
      z=280*(log(yp)/log(yo));
```

```
     _settextposition (20.9*z/280,9);sprintf
(buf1,"%1.3f",yp);_outtext(buf1);}}
     for (xp=0;xp<=1;xp+=.1){_settextposition (22,14+65*xp);
     sprintf (buf1,"%1.2f",xp*D*W*L/(Q*B));_outtext(buf1);}
     _setcolor(14);_settextcolor(11);_moveto(110,0);
     for (i=0;i<=N;i++){hx=(float)i/STZ;
     xp=110+(hx)*529;yp=277*(log(cb[i])/log(yo));
     _lineto (xp,yp);}_settextcolor(14);
      _settextposition (15,16);_outtext ("Eff = ");_settextcolor(11);sprintf
(buf1,"%2.2f",100*(1-cb[N]));_outtext(buf1);_outtext("%");
     _settextcolor(14);_settextposition (16,16);_outtext ("Intercept =
");_settextcolor(11);sprintf (buf1,"%1.4f",in);_outtext(buf1);
     _settextposition (24,1);_outtext ("(p)lotter prin(t)er prn(s)crn (m)enu or
(e)xit ?");
     _settextcolor(12);for (i = 163; i<640; i += 53){
     _putimage (i,277,buffer,_GOR);}
     for (j=1;j<=nd;j++){dy=yo*pow(10,j-1);
     for (yp=yo*pow(10,j-1);yp<=yo*pow(10,j);yp+=dy){
     z=277*(log(yp)/log(yo));_putimage (110,z,buffer,_GOR);}}
out: while(!kbhit());resp[0]=getch();resp[0]=tolower(resp[0]);
     switch (resp[0]){
     case 's':
          prnscrn();
          goto out;
     case 'p':
          hp();
          goto out;
     case 't':
          print();
          goto out;
     case 'm':
     default:
          printf ("program complete"); }
     _setvideomode (_DEFAULTMODE);
     return (0);
}
```

```
hp()
{
     int px1=1700;int px2=8175;int py1=1520; int py2=7350;
     stream = fopen("COM1","wr");
     setvbuf(stream,buf,_IOFBF,sizeof(buf));
     fprintf (stream,"\33%s",".N;19:");
     fprintf (stream,"\33%s",".H180;;17:");
     fprintf (stream,"%s","IN;SP1;VS25;");
     fprintf (stream,"IP1700,1520,8175,7350;");if(dsn>0){yo=yo1;goto mult;}
     fprintf (stream,"%s %d %d","PUPA",px1,py1);hand();
     fprintf (stream,"%s %d %d %d %d %d %d %d %d %d
%d","PDPA",px1,py1,px1,py2,px2,py2,px2,py1,px1,py1);hand();
     fprintf (stream,"%s %d %d %d %d %d %d %d %d %d %d
%s","PDPA",px1-20,py1,px1-20,py2,px2,py2,px2,py1-20,px1,py1-20,";PU");hand();
     fprintf (stream, "SI.15,.25;tl2,0;sp2;");
     if (nd>=3){fprintf(stream,"SI.12,.20;");}
     for (j=1;j<=nd;j++){dy=yo*pow(10,j-1);
     for (yp=yo*pow(10,j-1);yp<=yo*pow(10,j);yp+=dy){ py1=(int)FNPY(yp);
     fprintf (stream,"%s %d %d %s %1.3f\3",
"tl2,0;PUPA",px1,py1,";YT;CP-6.5,0;LB",yp);hand();
     fprintf (stream,"%s %d %d %s","tl0,2;PUPA",px2,py1,";YT");hand();}}
     for (j=1;j<=nd;j++){dy=yo*pow(10,j-1);
     for (yp=yo*pow(10,j-1);yp<=yo*pow(10,j);yp+=dy/2){ py1=(int)FNPY(yp);
     fprintf (stream,"%s %d %d %s ", "tl1,0;PUPA",px1,py1,";YT");hand();
     fprintf (stream,"%s %d %d %s","tl0,1;PUPA",px2,py1,";YT");hand();}}
for (i=1;i<=9;i++){hx=(float)i/10;px1=(int)FNPX(hx);
     fprintf (stream,"%s %d %s %1.2f\3",
"tl2,0;PUPA",px1,"1520;XT;CP-1,-1;LB",(hx)*D*W*L/(Q*B));hand();}
     for (i=0;i<=50;i++){hx=(float)i/50;px1=(int)FNPX(hx);
     fprintf (stream,"%s %d %s","TL1,0;PUPA",px1,"1520;XT;");hand();}
     fprintf (stream,"%s\3","SP1;SI;PUPA4937,1520;CP-3,-3;LBDWL/QB");hand();
     fprintf (stream,"%s\3", "DIO,1;PUPA1700,4435;CP-2,3;LBC/Co");hand();
mult:     fprintf (stream, "SP2;IW1700,1520,8175,7350" );
     fprintf (stream, "PUPA1700,7350");
     for
(i=1;i<=N;i++){hx=(float)i/N;px1=(int)FNPX(hx);yp=cb[i];py1=(int)FNPY(yp);
```

```
     fprintf (stream,"%s %d %d","PDPA", px1,py1);hand();}
     fprintf (stream,
"SI.15,.25;DI;IW;PUPR25,0;UC0,6,99,1,1,2.2,-2.2,-.2,-4.8,-.2,4.8,2.2,3.2;");
     fprintf (stream,"%s %2.1E\3", "CP0,0;LB=",E);hand();
     if (dsn==0){fprintf (stream,"%s\3",
"SI;SP1;DI;PUPA4938,7350;CP-13,-2;LBAnnular Denuder");}
     fprintf (stream, "IW;PUPA0,0;SP0");
     fflush (stream);dsn=dsn+1;yo1=yo;
     fclose;
     return(0);
}
store()
{
     stream = fopen (fname, "w");
     fprintf
(stream,"%d\,%f\,%d\,%f\,%f\,%f\,%f\,%f\,%f\,%f\,%f\,%f\,%f",ST,STZ,N,L,B,W,Q,D,T,-
E,M,in);
     for (i=1;i<=7;i++){fprintf (stream,"\n\r%d",BFL[i]);}
     for (i=0;i<=N+1;i++){fprintf (stream,"\n\r%f",cb[i]);}
     fclose (stream);
     return(0);
}
print()
{
     header();
     fprintf(stream,"\n\r%s\n\r","z/L          Eff,%");
     for (i=0;i<=N;i++){fprintf(stream,"%1.4f %s %5.2f\n\r",(float)i/N,"
",100*(1-cb[i]));}
     fprintf(stream,"\014");fclose(stream);
     return(0);
}
FNPX()
{
     zz=1700+hx*6475;
     return (zz);
}
```

```
FNPY()
{
     zz=7350-5830*(log(yp)/log(yo));
     return (zz);
}
hand()
{
     int jk=0;
     while (jk<=10000){jk++;}
     return(0);
}

prnscrn()
{
     stream = fopen("LPT1","w");fprintf(stream,"\v\v\033\101\007");
     if (pr=='i'){fprintf(stream,"\033\062");}
     for(j=0;j<=320;j+=7){for(i=0;i<=639;i++){tm[i]=0;
     for(k=0;k<=7;k++){m[k]=_getpixel(i,k+j);if(m[k]>1){m[k]=1;}
     tm[i]=tm[i]+m[k]*pow(2,(7-k));}}
     fprintf (stream,"\v\r\t\033\114\200\002");for(i=0;i<=639;i++){
     fputc(toascii(tm[i]),stream);}
     }
     fprintf(stream,"\v\v\r");
     fprintf(stream,"\033\101\011");fprintf(stream,"\033\062");
     header();fprintf(stream,"\014");
     fflush(stream);
     fcloseall;return(0);
}
header()
{
     fprintf(stream,"                    Annular Denuder");
     fprintf(stream,"\n\r%s %4.0f %s\n\r","Flow Rate = " ,Q/16.667 ," L/min");
     fprintf (stream,"%s %3.1f %s\n\r","Length = ",L," cm");
     fprintf (stream, "%s %1.3f %s\n\r","D = ",D," cm^2/sec");
     fprintf (stream," %s %3.1f %s\n\r","T = ",T-273," C");
     fprintf (stream,"%s %3.0f\n\r","M = ",M);
```

```
    fprintf (stream,"%s %4.1f %s\n\r","Slit Width = ",W," cm");
    fprintf (stream,"%s %1.1e\n\r","Collision efficiency = ",E);
    fprintf (stream,"%s %3.1f %s\n\r", "Gap = ",B," cm");
    fprintf(stream,"%s %3.0f %s\n\r","Pressure = ",P*760," torr");
    fprintf(stream,"%s %3.2f\n\r","DWL/QB = ",D*W*L/(Q*B));
    NRE= Q*P*1.37e05/((W+2*B)*pow(T,1.75));
    fprintf(stream,"%s %4.0f\n\r","Reynolds number = ",NRE);
    if (BFL[1]==11){fprintf (stream," Laminar flow");}
    if (BFL[2]==11){fprintf (stream," Plug flow");}
    return(0);
}
```

APPENDIX B
PAH Sampling Data

The following general footnotes apply to each table in Appendix B:

(a) Columns 2-6, concentration in ng/m^3 at STP.

(b) D = sampler with denuder; ND = no denuder.

(c) Total = ND (Filter + PUF).

(d) Values shown in parenthesis represent questionable data.

Other special footnotes are shown at the bottom of each table.

TABLE B-1. PHASE DISTRIBUTION DATA(a): RUN NO.62485(e,f)

Chemical	Filter		PUF		Total(c)	Percentage of Total Chemical Found As		
	ND(b)	D(b)	ND(b)	D(b)		Vapor	Artifact	Vapor + Artifact
Phenanthrene	4.20	3.10	50.70	39.60	54.90	22	70	92
Anthracene	0.56	0.36	3.60	1.60	4.20	53	34	87
Fluoranthene	3.20	1.10	8.10	7.50	11.30	25	47	72
Pyrene	1.30	0.53	7.30	2.70	8.60	62	22	84
Cyclopenta(c,d)-pyrene	*(g)	*	*	*	*	*	*	*
Benzo(a)-anthracene	0.34	0.15	0.09	0.02	0.43	(60)(d)	(-40)	20
Chrysene	0.52	0.27	0.32	0.08	0.84	(58)	(-20)	38
Benz(e)pyrene	0.27	0.19	*	*	0.27	*	*	*
Benz(a)pyrene	0.28	0.22	*	*	0.28	*	*	*
Indeno(1,2,3-c,d)-pyrene	0.78	0.74	*	*	0.78	*	*	*
Benzo(g,h,i)-perylene	0.61	0.55	*	*	0.61	*	*	*
Coronene	*	*	*	*	*	*	*	

(e) Temperature Range = 16.0 to 31.0 C; Average Temperature = 23.8 C
(f) Total Particulate Loading = 69.5 ug/m^3
(g) * = not detectable

TABLE B-2. PHASE DISTRIBUTION DATA(a): RUN NO. 70185(e,f)

Chemical	Filter		PUF		Total(c)	Percentage of Total Chemical Found As		
	ND(b)	D(b)	ND(b)	D(b)		Vapor	Artifact	Vapor + Artifact
Phenanthrene	0.75	0.75	80.60	250.00	81.40	(see footnote h below)		(99)
Anthracene	0.15	0.13	2.30	92.00	2.50			(92)
Fluoranthene	0.60	0.71	15.30	25.40	15.90			(96)
Pyrene	0.31	0.35	4.60	21.20	4.90			(94)
Cyclopenta(c,d)-pyrene	*(g)	*	*	*				*
Benzo(a)-anthracene	0.17	0.09	0.05	0.19	0.22			(22)
Chrysene	0.22	0.19	0.25	0.62	0.47			(53)
Benz(e)pyrene	0.21	0.17	0.05	0.35	0.26			(19)
Benz(a)pyrene	0.19	0.13	0.02	0.11	0.21			(10)
Indeno(1,2,3-c,d)-pyrene	0.28	0.13	*	*	0.28			*
Benzo(g,h,i)-perylene	0.26	0.16	*	*	0.26			*
Coronene	0.27	0.13	*	*	0.27			*

(e) Temperature Range = 18.0 to 24.0 C; Average Temperature = 21.0 C
(f) Total Particulate Loading = 73.5 ug/m^3
(g) * = not detectable
(h) Contaminated PUF in denuder sampler, total of vapor plus artifact estimated from non-denuder sampler data.

TABLE B-3. PHASE DISTRIBUTION DATA(a): RUN NO. 71085(e,f)

Chemical	Filter		PUF		Total(c)	Percentage of Total Chemical Found As		
	ND(b)	D(b)	ND(b)	D(b)		Vapor	Artifact	Vapor + Artifact
Phenanthrene	0.72	0.56	145.90	31.90	146.60	78	22	100
Anthracene	0.07	0.05	2.30	1.80	2.40	22	75	97
Fluoranthene	0.68	0.54	12.10	5.10	12.80	56	38	94
Pyrene	0.30	0.25	9.20	2.40	9.50	72	25	97
Cyclopenta(c,d)-pyrene	*(g)	*	*	*	*	*	*	*
Benzo(a)-anthracene	0.15	0.15	0.39	0.26	0.54	24	48	72
Chrysene	0.22	0.14	0.39	0.21	0.61	43	21	64
Benz(e)pyrene	0.14	0.11	*	*	0.14	*	*	*
Benz(a)pyrene	0.06	0.04	*	*	0.06	*	*	*
Indeno(1,2,3-c,d)-pyrene	0.13	0.07	*	*	0.13	*	*	*
Benzo(g,h,i)-perylene	0.15	0.13	*	*	0.15	*	*	*
Coronene	0.16	0.14	*	*	0.16	*	*	*

(e) Temperature Range = 17.0 to 32.0 C; Average Temperature = 25.0 C
(f) Total Particulate Loading = 66.0 ug/m^3
(g) * = not detectable

TABLE B-4. PHASE DISTRIBUTION DATA(a): RUN NO.71685(e,f)

Chemical	Filter		PUF		Total(c)	Percentage of Total Chemical Found As		
	ND(b)	D(b)	ND(b)	D(b)		Vapor	Artifact	Vapor + Artifact
Phenanthrene	1.30	0.89	47.20	(h)	48.50	(h)	(h)	97
Anthracene	0.21	0.08	2.30	(h)	2.50	(h)	(h)	92
Fluoranthene	1.30	0.53	6.60	4.70	7.90	34	49	83
Pyrene	0.56	0.27	4.10	4.20	4.70	4	83	87
Cyclopenta(c,d)-pyrene	0.07	0.13	*(g)	*	0.07	*	*	*
Benzo(a)-anthracene	0.23	0.11	0.11	0.07	0.34	47	(-15)(d)	32
Chrysene	0.32	0.18	0.15	0.10	0.47	40.0	(-9)	31
Benz(e)pyrene	0.19	0.10	*	*	0.19	*	*	*
Benz(a)pyrene	0.08	0.04	*	*	0.08	*	*	*
Indeno(1,2,3-c,d)-pyrene	0.17	0.10	*	*	0.17	*	*	*
Benzo(g,h,i)-perylene	0.19	0.12	*	*	0.19	*	*	*
Coronene	0.05	*	*	*	0.05	*	*	*

(e) Temperature Range = 15.0 to 34.0 C; Average Temperature = 24.5 C
(f) Total Particulate Loading = 59.5 ug/m^3
(g) * = not detectable
(h) Interferent present

TABLE B-5. PHASE DISTRIBUTION DATA(a): RUN NO.71885(e,f)

Chemical	Filter		PUF		Total(c)	Percentage of Total Chemical As		
	ND(b)	D(b)	ND(b)	D(b)		Vapor	Artifact	Vapor + Artifact
Phenanthrene	1.40	1.00	138.00	84.20	139.40	39	60	99
Anthracene	0.15	0.11	5.40	2.20	5.60	58	39	97
Fluoranthene	1.10	0.90	15.40	7.40	16.50	50	44	94
Pyrene	0.49	0.43	7.00	5.30	7.50	23	69	92
Cyclopenta(c,d)-pyrene	0.13	0.16	*(g)	*	0.13	*	*	*
Benzo(a)-anthracene	0.29	0.28	0.09	*	0.38	(26)(d)	(-3)	23
Chrysene	0.36	0.34	0.19	0.13	0.55	18	20	38
Benz(e)pyrene	0.37	0.36	*	*	0.37	*	*	*
Benz(a)pyrene	0.13	0.14	*	*	0.13	*	*	*
Indeno(1,2,3-c,d)-pyrene	0.34	0.38	*	*	0.34	*	*	*
Benzo(g,h,i)-perylene	0.36	0.50	*	*	0.36	*	*	*
Coronene	0.14	0.12	*	*	0.14	*	*	*

(e) Temperature Range = 19.0 to 37.0 C; Average Temperature = 26.7 C
(f) Total Particulate Loading = 138.0 ug/m^3
(g) * = not detectable

TABLE B-6. PHASE DISTRIBUTION DATA(a): RUN NO.72385(e,f)

Chemical	Filter		PUF		Total(c)	Percentage of Total Chemical As		
	ND(b)	D(b)	ND(b)	D(b)		Vapor	Artifact	Vapor + Artifact
Phenanthrene	0.89	2.10	68.20	46.00	69.10	30	68	98
Anthracene	0.14	0.10	2.00	1.50	2.10	26	71	97
Fluoranthene	0.95	1.90	9.50	5.80	10.50	26	65	91
Pyrene	0.43	0.73	3.60	4.10	4.00	(-20)(d)	(110)	90
Cyclopenta(c,d)-pyrene	0.08	0.07	*(g)	*	0.08	*	*	*
Benzo(a)-anthracene	0.21	0.15	0.19	0.11	0.40	35	13	48
Chrysene	0.25	0.25	0.24	0.22	0.49	4	45	49
Benz(e)pyrene	0.27	0.16	*	*	0.27	*	*	*
Benz(a)pyrene	0.17	0.08	*	*	0.17	*	*	*
Indeno(1,2,3-c,d)-pyrene	0.32	0.14	*	*	0.32	*	*	*
Benzo(g,h,i)-perylene	0.37	0.17	*	*	0.37	*	*	*
Coronene	0.40	0.14	*	*	0.40	*	*	*

(e) Temperature Range = 14.0 to 34.0 C; Average Temperature = 23.0 C
(f) Total Particulate Loading = 87.0 ug/m^3
(g) * = not detectable

TABLE B-7. PHASE DISTRIBUTION DATA(a): RUN NO.72985(e,f)

Chemical	Filter		PUF		Total(c)	Percentage of Total Chemical As		
	ND(b)	D(b)	ND(b)	D(b)		Vapor	Artifact	Vapor + Artifact
Phenanthrene	0.60	0.65	83.20	48.40	83.80	41	58	99
Anthracene	0.08	0.07	2.50	2.40	2.60	4	92	96
Fluoranthene	0.60	0.69	11.70	6.60	12.30	41	54	95
Pyrene	0.30	0.35	4.20	4.40	4.50	(-6)(d)	(100)	94
Cyclopenta(c,d)-pyrene	0.08	0.11	0.02	*(g)	0.10	(-10)	(30)	20
Benzo(a)-anthracene	0.19	0.16	0.09	0.06	0.28	21	11	32
Chrysene	0.26	0.24	0.24	0.27	0.50	2	50	52
Benz(e)pyrene	0.25	0.25	*	*	0.25	*	*	*
Benz(a)pyrene	0.12	0.12	*	*	0.12	*	*	*
Indeno(1,2,3-c,d)-pyrene	0.24	0.22	*	*	0.24	*	*	*
Benzo(g,h,i)-perylene	0.32	0.30	*	*	0.32	*	*	*
Coronene	0.14	0.12	*	*	0.14	*	*	*

(e) Temperature Range = 22.0 to 37.0 C; Average Temperature = 29.0 C
(f) Total Particulate Loading = 91.5 ug/m^3
(g) * = not detectable

TABLE B-8. PHASE DISTRIBUTION DATA(a): RUN NO. 21086(e,f)

Chemical	Filter		PUF		Total(c)	Percentage of Chemical As		
	ND(b)	D(b)	ND(b)	D(b)		Vapor	Artifact	Vapor + Artifact
Phenanthrene	4.50	2.70	18.10	9.90	22.60	49	31	80
Anthracene	0.57	0.36	0.43	0.25	1.00	43	0.0	43
Fluoranthene	5.50	2.30	2.20	0.94	7.70	(64)(d)	(-36)	29
Pyrene	2.50	1.30	1.80	1.10	4.30	(49)	(-7)	42
Cyclopenta(c,d)pyrene	0.57	0.43	*(g)	*	0.57	*	*	*
Benzo(a)anthracene	1.50	0.89	0.07	0.10	1.57	(41)	(-37)	4
Chrysene	3.10	1.90	0.11	0.03	3.21	(44)	(-41)	3
Benz(e)pyrene	1.30	0.83	*	*	1.30	*	*	*
Benz(a)pyrene	0.68	0.36	*	*	0.68	*	*	*
Indeno(1,2,3,c,d)pyrene	1.50	0.94	*	*	1.50	*	*	*
Benzo(g,h,i)perylene	2.00	1.50	*	*	2.00	*	*	*
Coronene	1.40	1.30	*	*	1.40	*	*	*

(e) Temperature Range = -4.0 to -7.0 C; Average Temperature = -5.5 C
(f) Total Particulate Loading = 94.5 ug/m^3
(g) * = not detectable

TABLE B-9. PHASE DISTRIBUTION DATA(a): RUN NO. 21886(e,f)

Chemical	Filter		PUF		Total(c)	Percentage of Chemical As		
	ND(b)	D(b)	ND(b)	D(b)		Vapor	Artifact	Vapor + Artifact
Phenanthrene	2.30	3.20	95.80	63.80	98.10	35	62	98
Anthracene	0.57	0.56	18.50	6.40	19.07	71	26	97
Fluoranthene	2.80	2.70	35.10	14.80	37.90	60	33	93
Pyrene	2.00	1.70	23.40	12.40	25.40	49	43	92
Cyclopenta(c,d)pyrene	2.10	1.70	0.37	0.32	2.47	(20)(d)	(-5)	15
Benzo(a)anthracene	4.50	2.40	0.91	0.51	5.41	(51)	(-35)	17
Chrysene	4.40	3.10	1.80	1.10	6.20	(36)	(-7)	29
Benz(e)pyrene	2.50	1.50	*(g)	*	2.50	*	*	*
Benz(a)pyrene	2.20	1.10	*	*	2.20	*	*	*
Indeno(1,2,3,c,d)pyrene	3.90	1.80	*	*	3.90	*	*	*
Benzo(g,h,i)perylene	3.80	2.00	*	*	3.80	*	*	*
Coronene	2.90	1.70	*	*	2.90	*	*	*

(e) Temperature Range = 10.0 to 17.0 C; Average Temperature = 12.8 C
(f) Total Particulate Loading = 117.5 ug/m^3
(g) * = not detectable

TABLE B-10. PHASE DISTRIBUTION DATA(a): RUN NO. 22586(e,f)

Chemical	Filter		PUF		Total(c)	Percentage of Chemical As		
	ND(b)	D(b)	ND(b)	D(b)		Vapor	Artifact	Vapor + Artifact
Phenanthrene	10.10	6.10	73.40	24.50	83.50	70	18	88
Anthracene	1.50	1.00	4.10	1.60	5.60	60	14	73
Fluoranthene	13.80	7.40	11.30	6.90	25.10	(48)(d)	(-3)	45
Pyrene	8.60	4.60	5.80	3.70	14.40	(47)	(-7)	40
Cyclopenta(c,d)pyrene	3.70	3.00	*(g)	*	3.70	*	*	*
Benzo(a)anthracene	6.90	5.00	0.11	0.10	7.01	(30)	(-29)	2
Chrysene	11.10	7.90	0.35	0.25	11.45	(32)	(-29)	3
Benz(e)pyrene	4.60	3.10	*	*	4.60	*	*	*
Benz(a)pyrene	3.30	2.30	*	*	3.30	*	*	*
Indeno(1,2,3,c,d)pyrene	4.80	3.50	*	*	4.80	*	*	*
Benzo(g,h,i)perylene	6.20	4.80	*	*	6.20	*	*	*
Coronene	4.00	3.20	*	*	4.00	*	*	*

(e) Temperature Range = -4.0 to 2.0 C; Average Temperature = -1.0 C
(f) Total Particulate Loading = 114.0 ug/m^3
(g) * = not detectable

TABLE B-11. PHASE DISTRIBUTION DATA(a): RUN NO. 30386(e,f)

Chemical	Filter		PUF		Total(c)	Percentage of Chemical As		
	ND(b)	D(b)	ND(b)	D(b)		Vapor	Artifact	Vapor +Artifact
Phenanthrene	5.70	2.00	84.80	32.80	90.50	68	25	94
Anthracene	0.86	0.36	7.10	0.99	7.96	(92)(d)	(-3)	89
Fluoranthene	5.50	1.80	15.00	7.40	20.50	61	12	73
Pyrene	2.40	0.91	12.10	5.70	14.50	60	23	83
Cyclopenta(c,d)pyrene	0.63	0.46	*(g)	*	0.63	*	*	*
Benzo(a)anthracene	1.00	0.68	0.48	0.27	1.48	(40)	(-7)	32
Chrysene	2.50	1.60	1.40	0.68	3.90	(46)	(-10)	36
Benz(e)pyrene	0.86	0.79	*	*	0.86	*	*	*
Benz(a)pyrene	0.37	0.35	*	*	0.37	*	*	*
Indeno(1,2,3,c,d)pyrene	0.92	0.73	*	*	0.92	*	*	*
Benzo(g,h,i)perylene	1.80	1.50	*	*	1.80	*	*	*
Coronene	1.60	1.20	*	*	1.60	*	*	*

(e) Temperature Range = 2.0 to 4.0 C; Average Temperature = 3.0 C
(f) Total Particulate Loading = 74.5 ug/m^3
(g) * = not detectable

TABLE B-12. PHASE DISRIBUTION DATA(a): RUN NO.30686(e,f)

Chemical	Filter		PUF		Total(c)	Percentage of Chemical As		
	ND(b)	D(b)	ND(b)	D(b)		Vapor	Artifact	Vapor + Artifact
Phenanthrene	4.70	3.60	59.30	30.60	64.00	52	41	93
Anthracene	0.56	0.41	1.60	0.65	2.16	57	17	74
Fluoranthene	5.00	3.00	9.70	5.40	14.70	48	18	66
Pyrene	2.40	1.60	4.60	3.00	7.00	38	28	66
Cyclopenta(c,d)pyrene	0.75	0.34	*(g)	*	0.75	*	*	*
Benzo(a)anthracene	1.60	0.79	0.23	0.20	1.83	(51)(d)	(-38)	13
Chrysene	2.50	1.20	0.43	0.45	2.93	(49)	(-34)	15
Benz(e)pyrene	1.00	0.55	*	*	1.00	*	*	*
Benz(a)pyrene	0.75	0.33	*	*	0.75	*	*	*
Indeno(1,2,3,c,d)pyrene	1.00	0.68	*	*	1.00	*	*	*
Benzo(g,h,i)perylene	1.30	0.90	*	*	1.30	*	*	*
Coronene	0.86	0.73	*	*	0.86	*	*	*

(e) Temperature Range = -8.0 to 1.5 C; Average Temperature = -2.0 C
(f) Total Particulate Loading = 81.5 ug/m^3
(g) * = not detectable

TABLE B-13. PHASE DISTRIBUTION DATA(a): RUN NO. 31186(e,f)

Chemical	Filter		PUF		Total(c)	Vapor	Artifact	Vapor + Artifact
	ND(b)	D(b)	ND(b)	D(b)				
Phenanthrene	6.70	2.80	94.90	42.20	101.60	62	32	93
Anthracene	0.98	0.62	5.90	2.70	6.88	57	28	86
Fluoranthene	7.70	3.00	17.70	8.00	25.40	63	7	70
Pyrene	4.10	1.70	10.40	5.30	14.50	57	14	72
Cyclopenta(c,d)pyrene	1.30	0.95	0.52	0.23	1.82	(39)(d)	(-11)	29
Benzo(a)anthracene	2.90	1.80	0.86	0.86	3.76	(33)	(-10)	23
Chrysene	4.90	2.90	*(g)	*	4.90	*	*	*
Benz(e)pyrene	1.90	1.30	*	*	1.90	*	*	*
Benz(a)pyrene	1.30	0.95	*	*	1.30	*	*	*
Indeno(1,2,3,c,d)pyrene	1.90	1.30	*	*	1.90	*	*	*
Benzo(g,h,i)perylene	2.60	1.90	*	*	2.60	*	*	*
Coronene	1.60	1.20	*	*	1.60	*	*	*

(e) Temperature Range = 3.0 to 10.0 C; Average Temperature = 4.8 C
(f) Total Particulate Loading = 106 ug/m^3
(g) * = not detectable

TABLE B-14. PHASE DISTRIBUTION DATA(a): RUN NO. 21688(e,f)

Compound	Filter		PUF		Total(c)	Percentage of Total Chemical Found As		
	ND(b)	D(b)	ND(b)	D(b)		Vapor	Artifact	Vapor + Artifact
Naphthalene	0.81	0.45	89.58	177.10	90.39	(-99)(d)	(198)	99
Quinoline	1.63	0.88	4.17	2.50	5.80	43	29	72
Acenaphthylene	0.18	0.13	2.29	1.58	2.47	32	61	93
Anthracene	0.63	0.48	1.17	0.50	1.80	48	17	65
Phenanthrene	6.46	3.75	41.67	41.67	48.13	6	81	87
Pyrene	5.00	3.13	2.02	1.38	7.02	(38)	(-9)	29
Fluoranthene	8.33	5.00	3.54	2.50	11.87	(39)	(-9)	30
Cyclopenta(c,d)pyrene	0.27	0.33	*(g)	*	0.27	*	*	*
Benz(a)anthracene	2.29	1.35	0.04	0.05	2.33	(43)	(-41)	2
Chrysene	3.54	2.29	0.13	0.18	3.67	(35)	(-31)	4
Retene	0.31	0.18	0.16	0.16	0.47	30	4	34
Benzo(a)pyrene	2.71	1.98	*	*	2.71	*	*	*
Benzo(e)pyrene	2.50	1.58	*	*	2.50	*	*	*
Benzofluoranthene	6.67	3.96	*	*	6.67	*	*	*
Perylene	0.52	0.27	*	*	0.52	*	*	*
Benzo(g,h,i)perylene	*	*	*	*	*	*	*	*
Indeno(1.2,3-c,d)pyrene	*	*	*	*	*	*	*	*
Coronene	*	*	*	*	*	*	*	*

(e) Temperature Range = -1.0 to 2.5 C; Average Temperature = 1.2 C
(f) Total Particulate Loading = 56.7 ug/m^3
(g) * = not detectable

TABLE B-15. PHASE DISTRIBUTION DATA(a): RUN NO. 30788(e,f)

Compound	Filter		PUF		Total(c)	Percentage of Total Chemical Found As		
	ND(b)	D(b)	ND(b)	D(b)		Vapor	Artifact	Vapor + Artifact
Naphthalene	0.77	0.37	43.01	35.55	43.78	18	80	98
Quinoline	1.83	0.87	0.30	0.09	2.13	(56)(d)	(-42)	14
Acenaphthylene	0.10	0.06	6.13	4.44	6.23	29	70	98
Anthracene	0.15	0.13	1.72	0.72	1.87	57	35	92
Phenanthrene	1.18	0.92	3.98	1.89	5.16	48	29	77
Pyrene	1.18	0.67	5.16	1.11	6.34	76	5	81
Fluoranthene	1.29	0.76	7.85	1.78	9.14	76	9	86
Cyclopenta(c,d)pyrene	4.09	0.38	*(g)	*	4.09	*	*	*
Benz(a)anthracene	0.65	0.48	0.05	0.07	0.70	(23)	(-16)	7
Chrysene	1.03	0.79	0.15	0.21	1.18	(16)	(-4)	13
Retene	0.13	0.06	0.49	0.16	0.62	69	10	79
Benzo(a)pyrene	0.55	0.60	*	*	0.55	*	*	*
Benzo(e)pyrene	0.65	0.69	*	*	0.65	*	*	*
Benzofluoranthene	1.40	1.56	*	*	1.40	*	*	*
Perylene	0.09	0.10	*	*	0.09	*	*	*
Benzo(g,h,i)perylene	0.87	1.01	*	*	0.87	*	*	*
Indeno(1,2,3-c,d)pyrene	0.58	0.63	*	*	0.58	*	*	*
Coronene	0.70	0.78	*	*	0.70	*	*	*

(e) Temperature Range = 2.5 to 12 C; Average Temperature = 5.6 C
(f) Total Particulate Loading = 79.4 ug/m^3
(g) * = not detectable

TABLE B-16. PHASE DISTRIBUTION DATA(a): RUN NO. 31088(e,f)

Compound	Filter		PUF		Total(c)	Percentage of Total Chemical Found As		
	ND(b)	D(b)	ND(b)	D(b)		Vapor	Artifact	Vapor + Artifact
Naphthalene	0.27	0.16	105.48	66.67	105.75	38	62	100
Quinoline	1.78	0.51	0.86	0.32	2.64	(70)(d)	(-38)	33
Acenaphthylene	0.10	0.06	10.27	6.80	10.37	35	64	99
Anthracene	0.27	0.23	1.51	0.80	1.78	44	41	85
Phenanthrene	2.74	1.60	24.66	17.33	27.40	32	58	90
Pyrene	2.47	1.27	3.15	1.60	5.62	51	5	56
Fluoranthene	3.01	1.60	4.79	2.53	7.80	50	12	61
Cyclopenta(c,d)pyrene	1.05	0.71	*(g)	*	1.05	*	*	*
Benz(a)anthracene	0.99	0.64	0.03	0.08	1.02	(31)	(-28)	3
Chrysene	1.37	1.11	0.11	0.17	1.48	(14)	(-7)	7
Retene	0.29	0.10	0.15	0.07	0.44	(66)	(-32)	34
Benzo(a)pyrene	0.78	0.83	*	*	0.78	*	*	*
Benzo(e)pyrene	0.99	0.85	*	*	0.99	*	*	*
Benzofluoranthene	2.05	1.87	*	*	2.05	*	*	*
Perylene	0.11	0.13	*	*	0.11	*	*	*
Benzo(g,h,i)perylene	1.25	1.17	*	*	1.25	*	*	*
Indeno(1,2,3-c,d)pyrene	0.74	0.72	*	*	0.74	*	*	*
Coronene	0.96	0.87	*	*	0.96	*	*	*

(e) Temperature Range = 1.0 to 5.8 C; Average Temperature = 3.4 C
(f) Total Particulate Loading = 61.0 ug/m^3
(g) * = not detectable

TABLE B-17. PHASE DISTRIBUTION DATA(a): RUN NO. 31588(e,f)

Compound	Filter		PUF		Total(c)	Percentage of Total Chemical Found As		
	ND(b)	D(b)	ND(b)	D(b)		Vapor	Artifact	Vapor + Artifact
Naphthalene	0.30	0.18	50.00	40.23	50.30	20	79	99
Quinoline	0.95	0.15	0.34	0.20	1.29	(75)(d)	(-49)	26
Acenaphthylene	0.49	0.02	3.16	0.24	3.65	(97)	(-10)	87
Anthracene	0.09	0.05	0.42	0.15	0.51	64	18	82
Phenanthrene	0.80	0.62	10.26	4.71	11.06	55	38	93
Pyrene	0.72	0.36	1.18	0.49	1.90	59	3	62
Fluoranthene	0.68	0.43	1.97	0.78	2.65	58	16	74
Cyclopenta(c,d)pyrene	0.12	0.11	*(g)	*	0.12	*	*	*
Benz(a)anthracene	0.18	0.15	0.03	0.02	0.21	(21)	(-6)	14
Chrysene	0.41	0.29	0.07	0.07	0.48	(27)	(-12)	15
Retene	0.10	0.04	0.07	0.06	0.17	(45)	(-4)	41
Benzo(a)pyrene	0.18	0.17	*	*	0.18	*	*	*
Benzo(e)pyrene	0.26	0.23	*	*	0.26	*	*	*
Benzofluoranthene	0.54	0.48	*	*	0.54	*	*	*
Perylene	0.02	0.02	*	*	0.02	*	*	*
Benzo(g,h,i)perylene	0.34	0.33	*	*	0.34	*	*	*
Indeno(1,2,3-c,d)pyrene	0.20	0.20	*	*	0.20	*	*	*
Coronene	0.32	0.30	*	*	0.32	*	*	*

(e) Temperature Range = -2.5 to -1.0 C; Average Temperature = -1.9 C
(f) Total Particulate Loading = 30.1 ug/m^3
(g) * = not detectable

TABLE B-18. PHASE DISTRIBUTION DATA(a): RUN NO. 31788(e,f)

Compound	Filter		PUF		Total(c)	Percentage of Total Chemical Found As		
	ND(b)	D(b)	ND(b)	D(b)		Vapor	Artifact	Vapor + Artifact
Naphthalene	1.25	0.49	80.00	63.95	81.25	21	77	98
Quinoline	0.49	0.00	2.38	0.11	2.87	(98)(d)	(-15)	83
Acenaphthylene	0.09	0.06	9.38	3.72	9.47	62	37	99
Anthracene	0.20	0.12	1.75	0.38	1.95	77	12	90
Phenanthrene	1.50	0.78	26.25	6.51	27.75	77	18	95
Pyrene	1.75	0.70	3.13	1.05	4.88	(67)	(-3)	64
Fluoranthene	1.88	0.79	4.38	1.40	6.26	68	2	70
Cyclopenta(c,d)pyrene	0.68	0.21	*(g)	*	0.68	*	*	*
Benz(a)anthracene	0.90	0.64	0.04	0.06	0.94	(27)	(-23)	4
Chrysene	1.25	0.97	0.10	0.15	1.35	(18)	(-11)	7
Retene	0.25	0.04	0.14	0.06	0.39	(79)	(-43)	36
Benzo(a)pyrene	0.48	0.34	*	*	0.48	*	*	*
Benzo(e)pyrene	1.00	0.84	*	*	1.00	*	*	*
Benzofluoranthene	2.13	1.86	*	*	2.13	*	*	*
Perylene	0.12	0.06	*	*	0.12	*	*	*
Benzo(g,h,i)perylene	1.50	1.28	*	*	1.50	*	*	*
Indeno(1,2,3-c,d)pyrene	0.88	0.76	*	*	0.88	*	*	*
Coronene	1.00	0.99	*	*	1.00	*	*	*

(e) Temperature Range = 1.5 to 5.0 C; Average Temperature = 3.5 C
(f) Total Particulate Loading = 84.9 ug/m^3
(g) * = not detectable

TABLE B-19. PHASE DISTRIBUTION DATA(a): RUN NO. 32188(e,f)

Compound	Filter		PUF		Total(c)	Percentage of Total Chemical Found As		
	ND(b)	D(b)	ND(b)	D(b)		Vapor	Artifact	Vapor + Artifact
Naphthalene	0.33	0.22	70.51	54.22	70.84	24	76	100
Quinoline	*(g)	*	0.36	0.22	0.36	40	60	100
Acenaphthylene	0.12	0.10	2.56	0.43	2.68	82	13	96
Anthracene	0.17	0.16	0.31	0.17	0.48	32	32	65
Phenanthrene	1.67	1.45	9.23	3.73	10.90	54	30	85
Pyrene	1.41	1.14	0.71	0.58	2.12	20	14	33
Fluoranthene	1.92	1.45	1.54	0.88	3.46	34	10	45
Cyclopenta(c,d)pyrene	0.28	0.04	*	*	0.28	*	*	*
Benz(a)anthracene	0.55	0.53	0.04	0.02	0.59	7	*	7
Chrysene	0.99	1.00	0.08	0.07	1.07	*	7	7
Retene	0.23	0.13	0.05	0.07	0.28	(30)(d)	(-12)	18
Benzo(a)pyrene	0.56	0.42	*	*	0.56	*	*	*
Benzo(e)pyrene	0.65	0.69	*	*	0.65	*	*	*
Benzofluoranthene	1.41	1.69	*	*	1.41	*	*	*
Perylene	0.08	0.03	*	*	0.08	*	*	*
Benzo(g,h,i)perylene	0.79	0.87	*	*	0.79	*	*	*
Indeno(1,2,3-c,d)pyrene	0.62	0.65	*	*	0.62	*	*	*
Coronene	0.83	0.84	*	*	0.83	*	*	*

(e) Temperature Range = -3.5 to 3.0 C; Average Temperature = -1.3 C
(f) Total Particulate Loading = 68.4 ug/m^3
(g) * = not detectable

TABLE B-20. PHASE DISTRIBUTION DATA(a): RUN NO. 51088(e,f)

Compound	Filter		PUF		Total(c)	Percentage of Total Found As		
	ND(b)	D(b)	ND(b)	D(b)		Vapor	Artifact	Vapor + Artifact
Naphthalene	0.19	0.22	5.73	15.87	5.92	(-173)(d)	(270)	97
Quinoline	0.27	0.61	1.64	0.52	1.91	41	45	86
Acenaphthylene	0.06	0.03	0.69	1.33	0.75	(-82)	(174)	92
Anthracene	0.17	0.30	11.82	6.67	11.99	43	56	99
Phenanthrene	1.09	2.06	218.18	112.70	219.27	48	51	100
Pyrene	1.00	1.11	11.82	5.08	12.82	53	39	92
Fluoranthene	1.64	1.75	22.73	10.63	24.37	50	43	93
Cyclopenta(c,d)pyrene	*(g)	*	*	*	*	*	*	*
Benz(a)anthracene	0.15	0.17	0.02	0.04	0.17	(-24)	(36)	12
Chrysene	0.32	0.28	0.09	0.14	0.41	(-3)	(24)	22
Retene	0.15	0.17	1.18	0.35	1.33	63	26	89
Benzo(a)pyrene	0.18	0.22	*	*	0.18	*	*	*
Benzo(e)pyrene	0.13	0.19	*	*	0.13	*	*	*
Benzofluoranthene	0.25	0.31	*	*	0.25	*	*	*
Perylene	(Not Analyzed during this run)							
Benzo(g,h,i)perylene	0.14	0.22	*	*	0.14	*	*	*
Indeno(1,2,3-c,d)pyrene	0.18	0.23	*	*	0.18	*	*	*
Coronene	0.14	0.23	*	*	0.14	*	*	*

(e) Temperature Range = 25.1 to 25.7 C; Average Temperature = 25.4 C
(f) Total Particulate Loading = 25.2 ug/m^3
(g) * = not detectable

TABLE B-21. DISTRIBUTION DATA(a): RUN NO. 51188(e,f)

Compound	Filter		PUF		Total(c)	Percentage of Total Chemical Found As		
	ND(b)	D(b)	ND(b)	D(b)		Vapor	Artifact	Vapor & Artifact
Naphthalene	0.38	0.23	32.39	29.87	32.77	8	91	99
Quinoline	0.45	0.32	3.52	0.84	3.97	72	17	89
Acenaphthylene	0.20	0.02	3.24	2.73	3.44	20	74	94
Anthracene	0.35	0.16	22.54	5.45	22.89	78	21	98
Phenanthrene	2.25	0.99	450.70	106.49	452.95	78	21	100
Pyrene	1.41	0.42	21.13	3.64	22.54	85	9	94
Fluoranthene	2.54	0.60	43.66	8.18	46.20	84	11	95
Cyclopenta(c,d)pyrene	0.17	0.12	*(g)	*	0.17	*	*	*
Benz(a)anthracene	0.37	0.29	0.05	0.03	0.42	(25)(d)	(-13)	12
Chrysene	0.46	0.17	0.12	0.09	0.58	(57)	(-37)	21
Retene	0.31	0.22	2.82	0.56	3.13	79	11	90
Benzo(a)pyrene	0.23	0.27	*	*	0.23	*	*	*
Benzo(e)pyrene	0.17	0.22	*	*	0.17	*	*	*
Benzofluoranthene	0.38	0.36	*	*	0.38	*	*	*
Perylene	(Not analyzed during this run.)							
Benzo(g,h,i)perylene	0.30	0.40	*	*	0.30	*	*	*
Indeno(1,2,3-c,d)pyrene	0.20	0.29	*	*	0.20	*	*	*
Coronene	0.30	0.40	*	*	0.30	*	*	*

(e) Temperature Range = 23.8 to 24.8 C; Average Temperature = 24.4 C
(f) Total Particulate Loading = 29.2 ug/m^3
(g) * = not detectable

TABLE B-22. PHASE DISTRIBUTION DATA(a): RUN NO. 60888(e,f)

Compound	Filter		PUF		Total(c)	Percentage of Total Chemical Found As		
	ND(b)	D(b)	ND(b)	D(b)		Vapor	Artifact	Vapor + Artifact
Naphthalene	0.12	0.13	11.21	7.26	11.33	36	63	99
Quinoline	0.52	0.62	1.03	0.11	1.55	55	11	66
Acenaphthylene	0.07	0.03	1.55	0.14	1.62	94	2	96
Anthracene	0.19	0.08	1.72	0.88	1.91	53	37	90
Phenanthrene	0.81	0.50	43.10	25.66	43.91	43	55	98
Pyrene	0.83	0.48	3.10	1.06	3.93	66	13	79
Fluoranthene	1.29	0.70	8.28	2.21	9.57	75	11	87
Cyclopenta(c,d)pyrene	0.17	0.16	*(g)	*	0.17	*	*	*
Benz(a)anthracene	0.42	0.27	0.01	0.01	0.43	(38)(d)	(-36)	2
Chrysene	0.66	0.50	0.10	0.08	0.76	(26)	(-13)	13
Retene	0.05	0.05	0.46	0.09	0.51	80	10	90
Benzo(a)pyrene	0.47	0.41	*	*	0.47	*	*	*
Benzo(e)pyrene	0.42	0.41	*	*	0.42	*	*	*
Benzofluoranthene	1.29	1.15	*	*	1.29	*	*	*
Perylene	(Not analyzed during this run.)							
Benzo(g,h,i)perylene	0.48	0.54	*	*	0.48	*	*	*
Indeno(1,2,3-c,d)pyrene	0.51	0.49	*	*	0.51	*	*	*
Coronene	0.33	0.36	*	*	0.33	*	*	*

(e) Temperature Range = 10.1 to 37.0 C; Average Temperature = 18.2 C
(f) Total Particulate Loading = 91.0 ug/m^3
(g) * = not detectable

TABLE B-23. PHASE DISTRIBUTION DATA(a): RUN NO. 61388(e,f)

Compound	Filter ND(b)	Filter D(b)	PUF ND(b)	PUF D(b)	Total(c)	Percentage of Total Chemical Found As: Vapor	Artifact	Vapor + Artifact
Naphthalene	0.35	0.28	4.04	3.60	4.39	12	80	92
Quinoline	0.92	0.36	0.40	0.22	1.32	(58)(d)	(-27)	30
Acenaphthylene	0.05	0.05	0.38	0.26	0.43	29	59	88
Anthracene	0.25	0.19	5.00	4.40	5.25	13	82	95
Phenanthrene	1.25	1.82	107.69	76.00	108.94	30	69	99
Pyrene	0.96	0.84	12.88	3.60	13.84	72	21	93
Fluoranthene	1.21	1.08	26.92	7.00	28.13	76	20	96
Cyclopenta(c,d)pyrene	0.19	0.06	*(g)	*	0.19	*	*	*
Benz(a)anthracene	0.35	0.15	0.04	0.05	0.39	(52)	(-42)	10
Chrysene	0.87	0.36	0.46	0.26	1.33	(57)	(-23)	35
Retene	0.37	0.28	2.88	0.36	3.25	87	2	89
Benzo(a)pyrene	0.48	0.28	*	*	0.48	*	*	*
Benzo(e)pyrene	0.44	0.28	*	*	0.44	*	*	*
Benzofluoranthene	1.06	0.60	*	*	1.06	*	*	*
Perylene	(Not analyzed during this run.)							
Benzo(g,h,i)perylene	0.58	0.34	*	*	0.58	*	*	*
Indeno(1,2,3-c,d)pyrene	0.60	0.30	*	*	0.60	*	*	*
Coronene	0.50	0.36	*	*	0.50	*	*	*

(e) Temperature Range = 23.4 to 40.3 C; Average Temperature = 32.1 C
(f) Total Particulate Loading = 88.4 ug/m^3
(g) * = not detectable

TABLE B-24. PHASE DISTRIBUTION DATA(a): RUN NO. 61488(e,f)

Compound	Filter ND(b)	Filter D(b)	PUF ND(b)	PUF D(b)	Total(c)	Percentage of Total Chemical Found As Vapor	Artifact	Vapor + Artifact
Naphthalene	0.25	0.20	18.52	21.70	18.77	(-17)(d)	(116)	99
Quinoline	0.46	0.42	5.56	1.32	6.02	73	19	92
Acenaphthylene	0.12	0.07	3.89	1.32	4.01	68	29	97
Anthracene	0.27	0.34	5.00	1.42	5.27	70	25	95
Phenanthrene	0.93	1.04	111.11	71.70	112.04	37	62	99
Pyrene	0.85	0.78	12.04	3.11	12.89	74	19	93
Fluoranthene	1.20	0.94	24.07	5.94	25.27	77	18	95
Cyclopenta(c,d)pyrene	0.67	0.63	*(g)	*	0.67	*	*	*
Benz(a)anthracene	0.56	0.43	0.16	0.22	0.72	10	12	22
Chrysene	1.11	0.77	0.83	0.57	1.94	33	10	43
Retene	0.15	0.16	1.76	0.24	1.91	85	7	92
Benzo(a)pyrene	0.88	1.04	*	*	0.88	*	*	*
Benzo(e)pyrene	1.20	1.32	*	*	1.20	*	*	*
Benzofluoranthene	3.33	3.40	*	*	3.33	*	*	*
Perylene	(Not analyzed during this run.)							
Benzo(g,h,i)perylene	1.47	1.89	*	*	1.47	*	*	*
Indeno(1,2,3-c,d)pyrene	1.01	1.23	*	*	1.01	*	*	*
Coronene	0.81	1.04	*	*	0.81	*	*	*

(e) Temperature Range = 22.8 to 42.2 C; Average Temperature = 30.4 C
(f) Total Particulate Loading = 113.5 ug/m^3
(g) * = not detectable

TABLE B-25. PHASE DISTRIBUTION DATA(a): RUN NO. 61588(e,f)

Compound	Filter		PUF		Total(c)	Percentage of Chemical Found As		
	ND(b)	D(b)	ND(b)	D(b)		Vapor	Artifact	Vapor + Artifact
Naphthalene	0.38	0.35	3.40	4.42	3.78	(-27)(d)	(117)	90
Quinoline	1.13	0.63	0.60	0.21	1.73	(53)	(-18)	35
Acenaphthylene	0.06	0.04	0.48	0.17	0.54	64	25	89
Anthracene	0.30	0.23	4.40	2.12	4.70	53	41	94
Phenanthrene	1.18	1.37	88.00	61.54	89.18	31	68	99
Pyrene	1.16	1.04	10.80	2.88	11.96	72	19	90
Fluoranthene	1.58	1.04	24.00	5.96	25.58	78	16	94
Cyclopenta(c,d)pyrene	0.22	0.16	*(g)	*	0.22	*	*	*
Benz(a)anthracene	0.44	0.27	0.06	0.07	0.50	(35)	(-23)	12
Chrysene	1.26	0.58	0.54	0.31	1.80	(55)	(-25)	30
Retene	0.22	0.16	2.20	0.25	2.42	90	*	91
Benzo(a)pyrene	1.00	0.48	*	*	1.00	*	*	*
Benzo(e)pyrene	1.06	0.46	*	*	1.06	*	*	*
Benzofluoranthene	3.00	1.25	*	*	3.00	*	*	*
Perylene	(Not analyzed during this run.)							
Benzo(g,h,i)perylene	1.42	0.67	*	*	1.42	*	*	*
Indeno(1,2,3-c,d)pyrene	1.18	0.58	*	*	1.18	*	*	*
Coronene	1.12	0.65	*	*	1.12	*	*	*

(e) Temperature Range = 26.2 to 37.3 C; Average Temperature = 33.0 C
(f) Total Particulate Loading = 146.4 ug/m^3
(g) * = not detectable

TABLE B-26. PHASE DISTRIBUTION DATA(a): RUN NO. 62288(e,f)

Compound	Filter		PUF		Total(c)	Percentage of Total Chemical Found As		
	ND(b)	D(b)	ND(b)	D(b)		Vapor	Artifact	Vapor + Artifact
Naphthalene	0.27	0.36	4.55	2.41	4.82	45	50	94
Quinoline	0.60	0.40	*(g)	0.33	0.60	*	*	*
Acenaphthylene	0.04	0.03	0.22	0.22	0.26	4	81	85
Anthracene	0.25	0.14	4.91	4.31	5.16	15	80	95
Phenanthrene	1.18	1.52	112.73	55.17	113.91	54	45	99
Pyrene	0.98	0.80	4.00	11.55	4.98	(-163)(d)	(243)	80
Fluoranthene	1.44	1.00	8.36	25.86	9.80	(-190)	(276)	85
Cyclopenta(c,d)pyrene	0.64	0.52	*	*	0.64	*	*	*
Benz(a)anthracene	0.76	0.53	0.12	0.19	0.88	(20)	(-7)	14
Chrysene	1.04	0.55	0.31	0.59	1.35	17	6	23
Retene	0.14	0.17	0.51	1.52	0.65	(-179)	(258)	78
Benzo(a)pyrene	0.87	0.62	*	*	0.87	*	*	*
Benzo(e)pyrene	0.75	0.55	*	*	0.75	*	*	*
Benzofluoranthene	1.82	1.28	*	*	1.82	*	*	*
Perylene	(Not analyzed during this run.)							
Benzo(g,h,i)perylene	0.85	0.86	*	*	0.85	*	*	*
Indeno(1,2,3-c,d)pyrene	0.89	0.79	*	*	0.89	*	*	*
Coronene	0.91	0.88	*	*	0.91	*	*	*

(e) Temperature Range = 33.4 to 38.8 C; Average Temperature = 36.3 C
(f) Total Particulate Loading = 103.3 ug/m^3
(g) * = not detectable

TABLE B-27. PHASE DISTRIBUTION DATA(a): RUN NO. 62388(e,f)

Compound	Filter		PUF		Total(c)	Percentage of Total Chemical Found As		
	ND(b)	D(b)	ND(b)	D(b)		Vapor	Artifact	Vapor + Artifact
Naphthalene	0.25	0.19	6.47	11.57	6.72	(-78)(d)	(174)	96
Quinoline	0.42	0.23	0.65	0.15	1.07	(67)	(-6)	61
Acenaphthylene	0.05	0.03	1.12	0.31	1.17	75	21	96
Anthracene	0.15	0.07	1.38	1.74	1.53	(-20)	(110)	90
Phenanthrene	0.76	0.68	37.93	41.32	38.69	(-9)	(107)	98
Pyrene	0.65	0.38	3.62	1.65	4.27	57	28	85
Fluoranthene	0.83	0.45	9.48	3.80	10.31	63	29	92
Cyclopenta(c,d)pyrene	0.24	0.18	*(g)	*	0.24	*	*	*
Benz(a)anthracene	0.36	0.21	0.04	0.04	0.40	(41)	(-31)	10
Chrysene	0.52	0.28	0.12	0.09	0.64	(46)	(-27)	19
Retene	0.04	0.04	0.33	0.07	0.37	77	12	89
Benzo(a)pyrene	0.41	0.32	*	*	0.41	*	*	*
Benzo(e)pyrene	0.47	0.37	*	*	0.47	*	*	*
Benzofluoranthene	1.03	0.70	*	*	1.03	*	*	*
Perylene	(Not analyzed during this run.)							
Benzo(g,h,i)perylene	0.84	0.76	*	*	0.84	*	*	*
Indeno(1,2,3-c,d)pyrene	0.59	0.42	*	*	0.59	*	*	*
Coronene	0.57	0.63	*	*	0.57	*	*	*

(e) Temperature Range = 15.1 to 38.5 C; Average Temperature = 22.7 C
(f) Total Particulate Loading = 48.2 ug/m^3
(g) * = not detectable